
1 **Genetic basis of rice ionomic variation revealed by Genome-wide association studies**

2

3 **Meng Yang^{a, 1}, Kai Lu^{a, 1}, Fang-Jie Zhao^b, Weibo Xie^a, Priya Ramakrishna^c,**
4 **Guangyuan Wang^a, Qingqing Du^a, Limin Liang^a, Cuiju Sun^a, Hu Zhao^a, Zhanyi**
5 **Zhang^a, Xin-Yuan Huang^b, Wensheng Wang^a, Huaxia Dong^a, Jintao Hu^a, Luchang**
6 **Ming^a, Yongzhong Xing^a, Gongwei Wang^a, Jinhua Xiao^a, David E. Salt^c, Xingming**
7 **Lian^{a, 2}**

8

9 ^aNational Key Laboratory of Crop Genetic Improvement and National Center of Plant
10 Gene Research (Wuhan), Huazhong Agricultural University, Wuhan, China

11 ^bState Key Laboratory of Crop Genetics and Germplasm Enhancement, College of
12 Resources and Environmental Sciences, Nanjing Agricultural University, Nanjing, China

13 ^cCentre for Plant Integrative Biology, School of Biosciences, University of Nottingham,
14 Sutton Bonington Campus, Loughborough, United Kingdom

15 ¹These authors contributed equally to this work

16 ²Address correspondence to xmlian@mail.hzau.edu.cn

17

18

19 **Abstract**

20 Rice (*Oryza sativa*) is an important dietary source of both the essential micronutrients
21 and the toxic trace elements to humans. The genetic basis underlying the variations in the
22 mineral composition, the ionome, in rice remains largely unknown. Here, we describe a
23 comprehensive study of the genetic architecture of the variation in rice ionome by
24 performing genome-wide association study (GWAS) on the concentrations of 17 mineral
25 elements in rice grain from a diverse panel of 529 accessions each genotyped at
26 approximately 6.4 million SNPs. We identified 72 loci associated with natural ionic
27 variations, 32 of which are common across locations and 40 are common within location.
28 We have identified candidate genes for 42 loci and provide evidence for the causal nature
29 of three genes, *SKC1* for sodium, *Os-MOT1;1* for molybdenum and *Ghd7* for nitrogen.
30 Comparison of rice GWA mapping data with *Arabidopsis thaliana* also identifies the
31 well-known as well as new candidates with potential for further characterization. Our
32 study provides new insights into the genetic basis of ionic variations in rice, and
33 serves as an important foundation for further studies on the genetic and molecular
34 mechanisms controlling the rice ionome.

35

36 **Introduction**

37

38 Plants require at least 14 essential mineral nutrients and several beneficial elements for
39 growth, development and resistance to biotic and abiotic stresses (Marschner and
40 Marschner, 2012). Large quantities of macronutrient fertilizers [nitrogen (N), phosphorus
41 (P), potassium (K)] are used in modern agriculture to increase crop yields, often resulting
42 in adverse impacts on the environment (Withers and Lord, 2002). Increasing the use
43 efficiencies of macronutrient fertilizers is critical for environmental quality and
44 agricultural sustainability. Meanwhile, plants also take up non-essential and toxic
45 elements from the soil, which may cause phytotoxicity or enter the food chain posing a

46 risk to human health (Clemens et al., 2002; Williams and Salt, 2009). Cultivated rice
47 (*Oryza sativa* L.) is one of the most important crops that feed about half of the world's
48 human population. For people who consume rice as the staple food, rice is a major
49 dietary source of both the essential micronutrients [e.g. iron (Fe) and zinc (Zn)] and toxic
50 elements [e.g. cadmium (Cd) and arsenic (As)] (White and Broadley, 2009; Zhao et al.,
51 2010; Clemens and Ma, 2016). It has been estimated that up to two billion people
52 worldwide suffer from Fe and Zn deficiencies, particularly in the populations with
53 cereals as their staple food (White and Broadley, 2009; Swamy et al., 2016; Trijatmiko et
54 al., 2016), and also a large number of populations poisoning with Cd and As especially
55 for people in south Asian countries (Clemens and Ma, 2016; Chen et al., 2018).
56 Enhancing the accumulation of essential micronutrients and reducing the concentrations
57 of potentially toxic elements in rice grain are of fundamental importance for food quality
58 and human health.

59 The composition of mineral nutrients and trace elements in plants, defined as the
60 plant ionome (Lahner et al., 2003; Salt et al., 2008), is determined by the genetic,
61 environmental and developmental factors as well as their interactions. Many genes
62 responsible for the uptake, translocation and storage of mineral elements in plants have
63 been identified. Based on studies using bi-parental populations, a large number of QTLs
64 for mineral concentrations in rice have been reported (Lu et al., 2008; Garcia-Oliveira et
65 al., 2009; Norton et al., 2010; Norton et al., 2012a; Du et al., 2013; Zhang et al., 2014;
66 Mahender et al., 2016; Ohmori et al., 2016). To date, only a small number of the mineral
67 QTLs have been finely mapped, leading to the identification of the causal genes,
68 including *Os-HKT1;5* (or *SKC1*) for sodium (Na), *Os-HMA3* for Cd, *NRT1.1B* for N, and
69 *Os-HMA4* for copper (Cu) (Ren et al., 2005; Ueno et al., 2010; Miyadate et al., 2011; Hu
70 et al., 2015; Huang et al., 2016). However, the gene networks controlling mineral
71 accumulation and homeostasis are complex and largely remain to be elucidated (Lahner
72 et al., 2003). A pivotal task in plant ionomic research is to unravel the genetic basis

73 underlying the variations of the ionome among natural accessions of a plant species and
74 crop cultivars. This knowledge is essential not only for understanding how plants adapt
75 to their mineral environment, but also for potential exploitation of alleles for breeding
76 crop cultivars with improved nutrient use efficiencies and better quality.

77 Genome-wide association study (GWAS) is a powerful tool to unravel the molecular
78 basis for phenotypic diversity. It has the power to genetically map multiple traits and
79 provides a complementary strategy to classical mapping using bi-parental synthetic
80 recombinant populations for dissecting complex traits (Huang and Han, 2014). GWAS on
81 the ionic profiles of *Arabidopsis thaliana* accessions has led to the identifications of a
82 number of loci as well as genes related to mineral accumulations, such as *HKT1;1* for Na
83 (Baxter et al., 2010; Segura et al., 2012), *MOT1* for molybdenum (Mo) (Shen et al., 2012;
84 Forsberg et al., 2015), *HMA3* for Cd (Chao et al., 2012) and *HAC1* for As (Chao et al.,
85 2014). Rice landraces have evolved from their wild progenitors and show both high
86 genotypic and phenotypic diversity (Huang et al., 2010). It is therefore possible to
87 perform GWAS to identify the genetic basis of much of this phenotypic variation in rice.
88 A large number of traits in rice, including numerous agronomic characters and
89 metabolites, have been studied using GWAS (Huang et al., 2012a; Chen et al., 2014;
90 Matsuda et al., 2015; Yano et al., 2016). Extensive heritable variation is known to exist in
91 the rice grain ionome for 1763 rice accessions of diverse geographic and genetic origin
92 (Pinson et al., 2015), and GWAS has been attempted on the concentrations of four
93 minerals (As, Cu, Mo and Zn) in rice grain (Norton et al., 2014), eight elements [Zn, Fe,
94 manganese (Mn), Cu, P, calcium (Ca), K and magnesium (Mg)] in brown rice (Nawaz et
95 al., 2015) and on aluminum (Al) tolerance (Famoso et al., 2011). These studies show the
96 promise of GWAS for ionic traits, but they are limited by the low density of SNPs and
97 bias caused by severe population structure inherent in the diversity panel containing both
98 indica and japonica cultivars.

99 A common problem encountered in the studies of ionic QTLs is the large effect of

100 the environment, especially soil properties and conditions that affect mineral supply and
101 availability (Pinson et al., 2015; Huang and Salt, 2016), which may mask the genetic
102 variation or render QTLs unreproducible. It is therefore important to conduct ionomic
103 studies on rice diversity panels across different field conditions to help reveal both the
104 generic and environment-specific QTLs. Here, we describe a comprehensive study of the
105 rice ionome based on GWAS using 529 diverse rice accessions each genotyped at
106 approximately 6.4 million SNPs. The rice diversity accessions were grown under five
107 different field or nutrient conditions. Vegetative tissues at the heading and maturity stages
108 and rice grains were analyzed for 17 mineral elements [N, P, K, Ca, Mg, Fe, Mn, Mo,
109 boron (B), Cu, Zn, cobalt (Co), Na, Cd, As, lead (Pb) and chromium (Cr)] using
110 high-throughput inductively-coupled plasma mass spectrometry (ICP-MS). We have
111 identified a large numbers of significant marker-trait associations and multiple
112 potentially causal candidate genes, three of which we have further validated. We have
113 also compared rice and *A. thaliana* GWAS data and identified some conserved features of
114 the genetic architecture underlying ionomic variations across plant taxa. The study
115 provides new insights into the genetic basis of natural ionomic variations in cultivated
116 rice and important information for comparative ionomic mapping in other plant species.

117

118 **Results**

119 **Variations in the ionome among 529 cultivated rice accessions**

120 To investigate the variation in the ionome in cultivated rice, a population of 529
121 cultivated rice accessions representing large variations in the geographical origin, the
122 genetic diversity and the usefulness for rice improvement, was used in this study
123 (Supplemental Data set 1). As described in our previous works (Chen et al., 2014; Zhao
124 et al., 2014; Xie et al., 2015), this population has been sequenced using the Illumina
125 Hiseq 2000 system, generating a total of 6.7 billion reads. We included the sequences
126 from 950 rice varieties generated by Huang et al. (2012a) and selected SNPs with

127 missing rates of less than 20%. We obtained a total of 6,428,770 SNPs with a missing
128 data rate (SNP call rate) of approximately 0.38% for use in the present study.
129 Comparisons between the imputed genotypes and relevant high-quality genome
130 sequences in the database as well as our array-based genotypes showed a high accuracy
131 (>99%) of the imputed genotypes (Xie et al., 2015). The SNPs and imputed genotypes
132 can be queried at RiceVarMap; <http://ricevarmap.ncpgr.cn> (Zhao et al., 2014). Analysis of
133 the sequence data shows that the 529 accessions include 295 *indica*, 156 *japonica*, 46 *aus*
134 and 32 intermediate. Among the 295 *indica* accessions, 98, 105 and 92 accessions are
135 further grouped into *indica* I (IndI), *indica* II (IndII) and *indica* intermediate, respectively.
136 The 156 *japonica* accessions are further grouped into temperate *japonica* (TeJ, 91
137 accessions), tropical *japonica* (TrJ, 44 accessions) and *japonica* intermediate (21
138 accessions) (Supplemental Data set 1).

139 The ionome is influenced by genetic and environmental variations, and the
140 development stage (Salt et al., 2008). N and P are two major nutrients that have large
141 impacts on plant growth and development. In the present study, we first investigated the
142 variation in the rice ionome among 529 accessions grown in three adjacent paddy fields
143 in Wuhan varying in the status of N and P supply, including a normal field (NF) receiving
144 standard N and P fertilization, a low N field (LN) and a low P field (LP) where either N
145 or P fertilizers have been withdrawn for the last decade. The ionic compositions (N, P,
146 K, Ca, Mg, Fe, Mn, Mo, B, Cu, Zn, Co, Na, Cd, As, Pb and Cr) of the shoots at the
147 heading stage, straw and brown rice at maturity were determined.

148 We found that the scale of ionic variation depends on both the element and the
149 plant tissue, with the essential macronutrients [N, P, K, Ca, Mg, relative standard
150 deviations (RSD) varying between 10 – 38%] showing smaller variations than
151 micronutrients (Fe, Zn, Cu, Mn, B, RDS varying between 20 – 191%) or nonessential
152 trace elements (Cd, As, Co, Cr, Pb, RSD varying between 28 – 196%), and the
153 reproductive tissue (brown rice) showing smaller variations than the vegetative tissues

154 (shoots or straws) (Supplemental Figure 1 and Supplemental Table 1). The broad-sense
155 heritability (H^2) of the 17 elements, averaged across different field conditions and tissue
156 types, ranged from 0.31 to 0.88 (Supplemental Table 2), consistent with previous reports
157 that a significant portion of ionic variation has a genetic basis (Pinson et al., 2015).
158 Particularly, elements such as N, P, K, Mg, Mo, Zn, As and Cd showed high average H^2
159 (≥ 0.68). The ionic compositions were also influenced by N and P treatments. Low N
160 resulted in significant decreases in the concentrations of most elements, whilst low P also
161 led to lower concentrations of some elements (e.g. N, Na, Fe, As, Cd and Pb). In general,
162 LN had larger impact on rice ionome compared to LP as revealed by multivariate
163 analyses. Principal component analysis (PCA) based on shoot or straw ionome revealed a
164 reasonable separation of accessions between NF and LN field conditions but not between
165 NF and LP fields (Supplemental Figure 2). Similar to PCA results, hierarchical clustering
166 analysis based on shoot or straw ionome showed that accessions grown in NF or LN
167 fields were generally clustered together, while such clustering was not observed between
168 accessions from NF and LP fields (Supplemental Figure 3). *Indica* and *japonica* are two
169 main subspecies of cultivated rice showing significant diversity in genetic architecture. In
170 general, *japonica* accessions accumulated significantly higher levels of most elements
171 than *indica* accessions (Supplemental Table 3). Median concentrations of Na, Mn, Co, Zn,
172 and Mo in *japonica* accessions were consistently higher than those of *indica* accessions
173 in all three tissues under three field conditions, with Mo concentrations showing the
174 largest difference (1.4 – 3.9 times) (Supplemental Table 3). In contrast, median Cd
175 concentration in brown rice of *japonica* accessions was considerably lower than that of
176 *indica* accessions, which is in agreement with previous reports (Arao and Ae, 2003;
177 Uruguchi and Fujiwara, 2013; Pinson et al., 2015). The fact that the median shoot Cd
178 concentration at the heading stage was larger in *japonica* than in *indica* suggests a lower
179 translocation of Cd from the shoots to the grains in the former.

180 Fig. 1 summarizes the influence of field condition, plant tissue and subspecies

181 (*indica* versus *japonica*) on the ionome. The type of plant tissue has the most distinctive
182 effect on the ionome, with N, P, Mo, Cu and Cr being preferentially distributed to brown
183 rice and forming a cluster, and the other 12 elements in a second cluster showing an
184 opposite pattern. The brown rice ionome appears to be separated according to the
185 subspecies, whereas the ionomes of shoot and straw are separated by the N and P status
186 of the fields.

187 To investigate further the effects of environment on the rice ionome, we grew the
188 rice population at Youxian, Hunan province, for two consecutive years. The field site at
189 Youxian had a lower soil pH and a higher Cd concentration than the soil at Wuhan
190 (Supplemental Table 4). Ionomics analysis was conducted on both the vegetative tissue
191 and rice grain (dehusked) harvested at crop maturity. Similar to the results from the trials
192 at Wuhan, most mineral elements showed relatively high H^2 across the two years at
193 Youxian (Supplemental Table 5). The differences in the mineral concentrations between
194 *indica* and *japonica* subpopulations were also generally consistent between Youxian and
195 Wuhan sites (Supplemental Tables 3 and 6).

196

197 **Genetic basis of variations in the rice ionome**

198 Based on the ionomic and sequence data of 529 rice accessions, we performed GWAS in
199 in the *indica* and *japonica* subpopulations separately, using both simple linear regression
200 (LR) and a linear mixed model (LMM). Because LMM results in fewer false positives
201 (Huang et al., 2010), the GWAS results based on LMM are presented here. P values of
202 1.8×10^{-6} and 4.1×10^{-6} were set as the significance thresholds for *indica* and *japonica*
203 respectively, after Bonferroni correction. Before performing GWAS, the Box-Cox
204 procedure was used to normalize the elemental traits which were non-normally
205 distributed (Supplemental Figures 4 to 7). For each element, a series of SNPs in a defined
206 region with P values lower than the threshold were detected. Since the median distances
207 of linkage disequilibrium (LD) decay in *indica* and *japonica* of this rice population had

208 been revealed to be 93 kb and 171 kb, respectively (Xie et al., 2015), the significant
209 SNPs within a 300 kb region are considered to represent a locus, and the SNP with the
210 lowest *P* value in a locus is defined as the SNP in closest linkage to the causal gene.
211 Based on this criterion, a total of 41 loci (or associations) that were detected in at least
212 two field conditions for the same tissue of the same subpopulation at Wuhan and 14 loci
213 were in the two consecutive years at Youxian (Supplemental Data sets 2 and 3).
214 Moreover, 32 loci were scanned across the locations of Wuhan and Youxian
215 (Supplemental Data set 4) and 2 loci were detected in all five field trials. Out of the total
216 87 loci detected, 72 were unique (Figures 2 and 3, and Supplemental Figure 8). Of the 17
217 mineral elements analyzed, all 17 elements had at least one GWAS locus and 9 elements
218 had at least 4 loci.

219

220 **Functional interpretations of the ionome GWAS results**

221 The ionic loci identified by GWAS provide important clues for understanding the
222 genetic architecture of the observed variations in the rice ionome. To identify candidate
223 genes responsible for each ionic locus, we extracted all genes within 300 kb of the
224 most significant SNPs and considered their annotations, functions of homologous genes
225 and distance from the peak SNPs (Supplemental Data set 6 and Supplemental Figure 9).
226 By applying this approach, we obtained a list of genes that represent plausible candidates
227 for the causal gene for each of the loci controlling elemental concentrations in rice
228 (Supplemental Data set 7).

229 We chose 2 loci for further investigation with the aim of identifying the causal genes.
230 We found that *Os-HKT1;5* is close (~14 kb upstream) to the most significant SNP
231 (sf0111478828) of a Na related locus, which was detected at both Wuhan and Youxian
232 locations (Figures 4A and 4C, and Supplemental Data set 7). *Os-HKT1;5* is a Na
233 transporter which was previously isolated in rice by map-based cloning using parents of
234 Nona Bokra (a salt-tolerant *indica* variety) and Koshihikari (a susceptible elite *japonica*

235 variety) (Ren et al., 2005), suggesting that allelic variation in *Os-HKT1;5* explains the
236 phenotypic variation in salt tolerance in the two rice varieties. Furthermore, the study
237 showed that the phenotypic variation is caused by the difference in the transport activity
238 of *Os-HKT1;5* (Ren et al., 2005), not by the difference in the *Os-HKT1;5* expression
239 level. Based on our sequence data, we found 9 SNPs which result in 9 amino-acid
240 changes in the coding sequence of *Os-HKT1;5* (Figure 3C), including the four amino
241 acids which were suggested to be responsible for the functional difference between the
242 Nona Bokra and Koshihikari alleles at *Os-HKT1;5* (Ren et al., 2005). We investigated the
243 linkage relationship between these 9 SNPs and the most significant SNP at this locus.
244 Interestingly, only one SNP (sf0111461701) is in strong linkage with the peak SNP
245 (Figure 3D). This SNP displays a substitution at the 184th amino acid of *Os-HKT1;5*
246 (H184R) with the variation occurring mainly in the *indica* subspecies (Figure 3E). The
247 two allelic groups separated by the base type of this SNP showed significant difference in
248 the straw Na concentration in all three field conditions, with the T allele (corresponding
249 to H at the 184th position of amino acid) containing lower Na than the C allele
250 (corresponding to R at the 184th position of amino acid) (Figures 3F to 3J). Because the
251 above 9 SNPs are not closely linked with each other, there are likely to be more than two
252 types of *Os-HKT1;5* alleles. According to these 9 SNPs, there are 21 haplotypes of
253 *Os-HKT1;5* in all 1479 accessions [529 accessions used in this study and 950 accessions
254 sequenced by Huang et al. (2012a); Supplemental Figure 10]. Both the haplotypes of
255 *HKT1;5^{NB}* (*Os-HKT1;5* from Nona Bokra, designated as Hap2) and *HKT1;5^K*
256 (*Os-HKT1;5* from Koshihikari, designated as Hap3) were found in the accessions
257 (Supplemental Figure 11). In fact, only six haplotypes (from Hap1 to Hap6) exist in more
258 than 10 accessions among the 1479 accessions. We analyzed the Na concentrations of the
259 6 haplotypes in our collection. We found that the Hap2, which is the only haplotype
260 representing “H” amino acid at the 184th position, showed the lowest Na concentration in
261 straws compared to other haplotypes in each subpopulation (Figure 5). These results

262 suggested that Hap2 is the strongest allele in restricting Na accumulation in the shoots
263 and in Na tolerance. It has been suggested that Os-*HKT1;5* functions in the roots to
264 recycle Na out of the xylem to limit the translocation of Na to the shoot. Loss or reduced
265 function of Os-*HKT1;5* therefore leads to increased shoot Na concentration (Horie et al.,
266 2009). Taken together, our results indicate that H184R is likely the key substitution that
267 causes functional variation in Os-*HKT1;5*. Unlike its homologous gene *HKT1;1* in
268 *Arabidopsis thaliana* (Baxter et al., 2010), Hap2 of Os-*HKT1;5* shows no obvious
269 difference in the geographical distribution from other haplotypes (Supplemental Figure
270 11), which may be caused by the fact that rice is domesticated and therefore the link
271 between genotype and the environment is now lost. Interestingly, Os-*HKT1;5* is
272 relatively conserved in *japonica*, with most accessions (93.5%) possessing the weak
273 allele Hap3 (Supplemental Figure 10). Only one *japonica* accession has the Hap2 allele.
274 Therefore, the Hap2 allele of Os-*HKT1;5* has the potential to enhance salt tolerance of
275 *japonica*, as well as *indica* cultivars without this allele. Furthermore, IndII accessions
276 contained significantly lower Na concentrations in the shoots compared to other
277 subpopulations with the same Os-*HKT1;5* haplotype (Supplemental Figure 12),
278 regardless whether the Os-*HKT1;5* haplotype is strong or weak, suggesting that the IndII
279 accessions harbor additional genes involved in regulating Na accumulation.

280 Because SNP sf0800123053 is strongly associated with Mo concentration (Figures
281 6A and 6B), we investigated the causal gene for the locus. SNP sf0800123053 is located
282 37 kb from LOC_Os08g01120 (encoding a putative sulfate transporter and named
283 Os-MOT1;1), which is the closest orthologue of At-*MOT1* (a major Mo transporter in
284 *Arabidopsis*) (Tomatsu et al., 2007; Baxter et al., 2008). GUS staining driven by the
285 Os-*MOT1;1* promoter revealed that Os-*MOT1;1* was mainly expressed in the lateral roots,
286 with weak expression in leaf blade, leaf sheath, culm, node and grain (Supplemental
287 Figure 13). We obtained a knock-down mutant of Os-*MOT1;1* and found that the mutant
288 accumulated significantly lower concentrations of Mo in both roots and shoots than

289 wild-type plants (Supplemental Figure 14), supporting the suggestion that *Os-MOT1;1* is
290 the causal gene underlying this Mo locus. Within this locus, significant SNPs were found
291 almost exclusively in *indica* subpopulations. One of these SNPs, sf0800085089, was
292 found to land directly on the promoter region of *Os-MOT1;1* (Figure 6C). Moreover,
293 accessions separated by SNP sf0800085089 in *indica* (hereafter called Ind-C and Ind-T)
294 showed significant difference in straw Mo concentrations in all five field trials (Figures
295 6E to 6I), suggesting that *Os-MOT1;1* contributes to the variation of Mo concentration in
296 *indica*. The nucleotide diversity of *Os-MOT1;1* genomic sequence in *indica* was then
297 analyzed. Several SNPs or INDELS were found to show a close linkage to SNP
298 sf0800085089 ($r^2 > 0.65$) (Figure 6D). One INDEL locating at the 5' UTR of *Os-MOT1;1*
299 with a 10 bp insertion in the group Ind-C (higher Mo group) and one SNP locating at the
300 ORF of *Os-MOT1;1* resulting in one amino-acid change were found and confirmed by
301 fully sequencing 20 randomly selected *indica* accessions (Figure 5C). Additionally, the
302 fully sequenced data revealed a number of new variation sites in the promoter region
303 including two insertions of 999 bp and 226 bp fragments, and some deletions of short
304 fragments (Figures 6J, 6K and Supplemental Figure 15), but no additional variation was
305 found in the *Os-MOT1;1* coding sequence (Supplemental Figure 16). To test whether the
306 variations in the promoter region affect the expression level of *Os-MOT1;1* among the
307 *indica* accessions, the *Os-MOT1;1* transcript levels in the roots of 10 accessions each of
308 Ind-C and Ind-T groups were determined under both Mo sufficient and deficient
309 conditions. The Ind-C group with higher Mo concentration had significantly higher levels
310 of *Os-MOT1;1* transcript than the Ind-T group under both conditions (Figure 6L and 6M).
311 At least four variants were found in the *Os-MOT1;1* protein among the 529 rice
312 accessions (Figure 7A). To investigate whether there are functional differences among
313 these variants, we over-expressed the four *Os-MOT1;1* types in rice plants (*O. sativa* L.
314 ssp. *japonica* cv. Zhonghua 11) and selected 6 transgenic lines for each *Os-MOT1;1* type,
315 3 with relatively high expression and 3 with relatively low expression, for further study

316 (Figure 7B). We found that overexpression of *Os-MOT1;1* increased Mo concentration in
317 both roots and shoots in an expression level dependent manner (Figures 7C and 7D). The
318 relationships between the expression level and root Mo concentration were similar
319 among the four types of *Os-MOT1;1* over-expressors (Figure 7E). For shoot Mo
320 concentration, the type2 over-expressing plants appeared to be more effective than the
321 other three types, but there was no significant difference among types 1, 3 and 4, the
322 latter two types corresponding to the accessions of Ind-T and Ind-C, respectively (Figure
323 7F). Taken together, our evidence is consistent with *Os-MOT1;1* being the causal gene
324 for the Mo locus with the lead SNP sf0800123053, and that the variation in Mo
325 concentration is caused by the allelic variation in the promoter region leading to variable
326 expression of *Os-MOT1;1*.

327

328 **Comparative GWAS for ionomic traits between rice and *A. thaliana***

329 It has been suggested that natural ionomic variation in different species tends to be
330 controlled by genes from the same gene families (Huang and Salt, 2016). Over recent
331 years, GWAS has been extensively performed in *A. thaliana* and several significant
332 ionomic loci have been identified using a set of ~349 wild accessions (Baxter et al., 2010;
333 Chao et al., 2012; Chao et al., 2014; Forsberg et al., 2015). Comparing the rice ionomic
334 GWAS data described here with that previously obtained using *A. thaliana* should allow
335 us to explore more systematically to what degree the genetic architecture controlling
336 ionomic variation is conserved across taxa between rice and *A. thaliana*. This
337 comparative GWAS approach could also provide further evidence in support of candidate
338 genes. We reran the GWAS using the publically available leaf ionomic data from the set
339 of 349 *A. thaliana* accessions with an updated fully imputed SNPs dataset with
340 10,707,430 biallelic SNPs using an accelerated mixed model (AMM) (Seren et al., 2012).
341 The ionomic data used was composed of the leaf concentrations of Na, Ca, Mg, B, P, K,
342 Mn, Fe, Co, Cu, As, Zn, Cd and Mo. All significant SNPs ($-\log(p\text{-value}) > 5$) and
343 corresponding candidate genes were organized based on their p -values per phenotype and
344 listed in Supplemental Data set 10. As was shown previously (Baxter et al., 2010; Chao

345 et al., 2012; Chao et al., 2014; Forsberg et al., 2015), the leaf concentrations of Na, Cd,
346 As and Mo showed the strongest associations with causal genes that have been
347 established as *At-HKT1;1* (AT4G10310), *At-HMA3* (AT4G30120), *At-HAC1*
348 (AT2G21045), and *At-MOT1;1* (AT2G25680), respectively. We also newly found several
349 strong SNPs which are highly associated with leaf Co or Zn concentrations (p -value <
350 10^{-9}) (Supplemental Data set 8). The most highly associated SNP for the variation in leaf
351 Co concentration was at Chr5: 902186 ($-\log(p\text{-value}) = 29.08$) within ~1 kb of the gene
352 *IRON-REGULATED 2* (*At-IRGT2/FPN2*; AT5G03570). This gene has previously been
353 shown to control leaf Co concentration using linkage mapping in a bi-parental F2
354 population derived from the accessions of Columbia-0 and Ts-1 (collected in Tossa de
355 Mar, Spain) (Morrissey et al., 2009). In addition, a number of SNPs with $-\log(p\text{-value}) >$
356 5 for the leaf concentrations of Ca, Mg, B, P, K, Mn, Fe or Cu and candidate genes were
357 also identified (Supplemental Data set 8).

358 We then extracted all genes within 300 kb of the lead SNPs in the rice GWAS data for
359 each element to look for orthologous genes with candidates obtained from the *A. thaliana*
360 GWAS data, using PLAZA Comparative Genomics Platform (PLAZA v2.5) (Van Bel et
361 al., 2012; Tomcal et al., 2013). Only a total of 5 couples of orthologous genes were
362 obtained for associations with As, Mn, Mo and Na (Supplemental Data set 9). The rice
363 genes *Os-HKT1;5* and *Os-MOT1;1* associated with variation in rice shoot Na and Mo,
364 respectively, were found to be paired with *At-HKT1;1* and *At-MOT1* previously
365 determined to control the variation in these same elements in *A. thaliana* leaves. This
366 provides strong evidence that the variations in Na and Mo are governed by the same
367 genes across monocots and dicots. The comparative GWAS approach therefore also
368 provides a useful and independent method to further validate the role of candidate genes
369 identified using GWAS.

370

371 **Rice ionome is affected by the heading date**

372 Heading date is an important trait for the adaptation of rice plants to different growth
373 environments (Jung and Muller, 2009). In general, rice accessions with later heading date

374 have a longer vegetative phase and consequently a larger yield potential. To test whether
375 heading date influences the rice ionome, we analyzed the correlations between elemental
376 concentrations and heading dates (Supplemental Figure 17). We found significant
377 negative correlations between heading date and the concentrations of N, P, K, Ca, B, Cu,
378 Fe and As, in some of the three plant tissues or field conditions at Wuhan. In contrast,
379 there were significant positive correlations between heading date and Cd concentrations
380 in all tissues from all three field conditions, as well as with Pb and Mn concentrations in
381 some tissues and field conditions. The negative and positive correlations between
382 heading date and As and Cd, respectively, were also observed in a panel of 467 locally
383 adapted rice cultivars in south China (Duan et al., 2017).

384 Nitrogen is one of the most important nutrients limiting crop productivity, whereas
385 overuse of N fertilizers can cause serious environmental damages. Increasing N use
386 efficiency in crops is therefore an important goal to enhance agricultural sustainability.
387 The locus defined by SNP sf0709172004 was found to be strongly associated with the
388 concentrations of N in shoots at heading stage, whilst the nearby SNP sf0709177919
389 defined the locus for heading date (Figures 8A and 8B). Furthermore, the locus
390 associated with N concentrations was still detected when heading date was used as a
391 covariate (Figure 8C). We therefore selected this locus for further analysis. We found that
392 the gene LOC_Os07g15770, known as *Hd4* or *Ghd7* and having a large effect on rice
393 heading date, is located at this locus (~17 kb away from the lead SNP) (Xue et al., 2008).
394 Because N concentration is strongly correlated with heading date (Supplemental Figure
395 17), we suggested that *Ghd7* is a likely candidate. According to the sequence data, there
396 are 45 haplotypes of *Ghd7* in all 529 accessions (Supplemental Data set 10). Within the
397 *indica* accessions there are 5 main haplotypes (Hap1~Hap5) (Figures 8D, 8E and
398 Supplemental Data set 10), among which Hap2 showed significantly shorter heading date
399 but higher N concentrations than other haplotypes (Figure 8F and 8G). In fact, the
400 nucleotide diversity of *Ghd7* genomic sequence had ever been analyzed in 104 rice

401 accessions and 58 of which were included in our collection (Lu et al., 2012;
402 Supplemental Data set 10). Consistent with our findings, haplotypes of *Ghd7* with longer
403 heading dates showed relatively lower N concentrations in shoots. To investigate the
404 effect of *Ghd7*, we compared N concentrations and heading dates among four
405 near-isogenic lines (NIL) developed previously in the genetic background of Zhenshan
406 97 with the introgressed segment around the *Ghd7* region from different rice varieties
407 (Xue et al., 2008). Three lines containing functional alleles of *Ghd7* [NIL(mh7),
408 NIL(nip7) and NIL(tq7)] contained significantly lower N concentrations in various
409 tissues than the line NIL(zs7) carrying a complete deletion in the corresponding region
410 (Figures 9A to 9C). Furthermore, overexpressing a functional allele (mh7) of *Ghd7* with
411 the ubiquitin promoter into Zhenshan 97 generally decreased N concentrations in shoots,
412 straw and brown rice compared with wild-type (Figures 9D to 9F).

413

414 **Loci involved in rice growth under low N or low P conditions**

415 It has been suggested that N uptake explained most of the variation for nitrogen use
416 efficiency (NUE) and grain yield at low N supply (Hirel et al., 2007). Variation in plant
417 biomass production at low N or low P supply reflects the variation in the abilities to
418 tolerate low N or low P, which are important traits for breeding rice cultivars that can
419 produce acceptable levels of yield with reduced fertilizer inputs. In the present study, we
420 found large variations among rice accessions in both the above-ground biomass and grain
421 yield under low N or low P conditions (Supplemental Figure 18). We performed GWAS
422 on above-ground biomass at both the heading and mature stages and grain yield. In our
423 collection, biomass at both heading and mature stages correlated negatively with N
424 concentrations but positively with the total amount of N in the plant (Supplemental
425 Figure 19). Grain yield also correlated positively with total N of the plant, especially in
426 the LN field. Loci that were associated with variation in biomass and grain yield at low N
427 field are likely to be involved in controlling rice growth under low N fertilization. We

428 explored the loci identified from at least two traits (for instance, biomass at heading stage
429 and grain yield) at low N field, low P field as well as normal field at Wuhan, respectively
430 (Supplemental Table 7). Meanwhile, loci which were identified in the same tissue and
431 subpopulation in at least two fields for each trait were also obtained. Based on the above
432 criteria, we obtained 11 loci responsible for biomass and grain yield (Supplemental Table
433 7). Of these loci, two are co-located with either Ghd7 or DTH8/Ghd8, which are known
434 to control the variation in biomass and grain yield (Xue et al., 2008; Wei et al., 2010; Yan
435 et al., 2011). Interestingly, we found that 5 loci were exclusively detected in the LN or
436 normal field whereas only 2 loci were common in both fields, suggesting different
437 genetic basis for controlling biomass production under low N and normal field condition.
438 In contrast, LP field shared all loci with normal or LN field. Furthermore, a locus defined
439 by SNP sf1125356264 was found from all 3 field conditions, which may contribute to
440 variations of biomass or grain yield under various N or P fertilization conditions.

441

442 **Genetic basis of low N and low P affecting ionome**

443 As described above, the concentrations of many elements were greatly affected by the N
444 or P status (Supplemental Figure 1 and Supplemental Table 1). This may reflect the
445 crosstalk between N or P and other elements and the adjustment of the ionome in
446 response to low N or low P conditions. Moreover, as essential macronutrients, N or P
447 deficiency may affect the transcription levels of many genes and alter root morphology
448 (Hermans et al., 2006). It is likely that these effects are genotype dependent. Therefore,
449 investigating the genetic basis of changing ionic profile at low N or low P conditions
450 may provide some clues to understanding the responses of ionome to the environment.

451 Based on the GWAS results of the rice ionome performed above, we extracted 32
452 loci associated with the concentrations of 11 elements (Supplemental Data set 11), which
453 were scanned across at least two tissues in one field condition. It is interesting that the
454 majority of these loci (19 of 32) were also common in two or more field conditions. In

455 contrast, 13 loci were specific to field conditions, including 7 for normal field, 5 for low
456 N field and 1 for low P field, Identification of the causal genes underlying these loci
457 would provide insights into how N and P impact the rice ionome, and would also benefit
458 rice breeding that tailor the varieties to local conditions.

459

460 **Discussion**

461 As an essential component of all living systems, the natural ionic variation has
462 significance in evolution and adaptation (Lahner et al., 2003; Huang and Salt, 2016).
463 Over the last decade, numerous genes and gene networks have been shown to be
464 involved in controlling mineral nutrient and trace element homeostasis in plants.
465 However, the loci that control natural ionic variation are still largely unknown,
466 especially in rice. By performing GWAS on the concentrations of 17 elements in
467 different tissues of 529 rice accessions grown under different locations, years and field
468 conditions, we have identified 72 locus-element associations with high reproducibility
469 across plant tissues, growth stages and field conditions (Supplemental Data sets 2 to 5).
470 Our study represents the most comprehensive GWAS of the rice ionome to date.

471 GWAS of the rice ionome has to overcome a number of limiting factors, including
472 the relatively small variation in plant elemental concentrations because of the
473 homeostasis of essential mineral nutrients and the usually large environmental variation.
474 Consistent with previous reports on *A. thaliana* (Baxter et al., 2012) and rice (Pinson et
475 al., 2015), we found that trace elements, especially the non-essential toxic elements,
476 showed greater variations than macronutrients in rice tissues (Figure 1 and Supplemental
477 Table 1), suggesting that the latter are more tightly regulated. It is possible that plants
478 have evolved stronger mechanisms to control the internal fluctuation of essential
479 nutrients, especially macronutrients (e.g. N, P, K), than for non-essential elements,
480 because the concentrations of macronutrients need to be maintained within relatively
481 narrow ranges that are optimal for growth and development. For non-essential elements

482 there would be little selection pressure to control their concentrations until they reach the
483 levels of toxicity. Despite different ranges of variation, 13 of the 17 elements determined
484 in our study were found to have a relatively high heritability within the same location
485 (average $H^2 \geq 0.5$) (Supplemental Table 2 and 5), indicating a good genetic basis for their
486 variations in agreement with previous studies on both *A. thaliana* and rice (Baxter et al.,
487 2012; Pinson et al., 2015). In contrast, elements including B, Fe, Cr and Pb showed low
488 heritability; the latter three elements are known to be prone to small soil or dust
489 contamination inflating their concentrations in plant tissues. However, the heritability for
490 most elements was lower when plants were grown at different locations (Supplemental
491 Table 5), consistent with previous studies that genetic variation of elements was
492 relatively strong across years at the same field location but relatively weak between field
493 locations (Norton et al., 2012b). To overcome the limitations associated with genetic
494 versus environmental variations, we conducted five field trials across different locations
495 and years and analyzed ionic profiles of different rice tissues of 529 rice accessions.
496 This approach allowed us to identify loci that are reproducible across environments
497 (Norton et al., 2012b; Norton et al., 2014). We obtained 32 loci (out of 72) that were
498 common across field locations (Supplemental Data sets 2 to 4). Moreover, 37 loci are
499 close to the QTLs associated with specific elemental concentrations in rice reported in
500 previous studies using bi-parental crosses or association mapping (Supplemental Data set
501 5). These loci represent genetic variations that are stable across different environments
502 and would be more useful for breeding purposes.

503 The high density of SNPs (~17 SNPs per kb in average) in our GWAS panel also
504 facilitates high-resolution mapping. The resolution (within approximately 100 kb) (Si et
505 al., 2016) is much higher than the loci generally defined with the interval QTL mapping
506 approach (Supplemental Data set 5). Because of the slow LD decay in rice and relatively
507 complex genetic architecture of elemental traits (Huang and Han, 2014), a locus in rice
508 identified by GWAS typically covers more than 20 genes (Matsumoto et al., 2005).

509 Using the information of functional gene annotation or their orthologous genes in other
510 plant species, plausible candidate genes for a number of loci identified by GWAS could
511 be established (Supplemental Data set 7). We further provide strong evidence that
512 *Os-HKT1;5* and *Os-MOT1;1* are the causal genes for the loci with the lead SNP
513 sf0111478828 and sf0800123053, respectively, which cause variations in Na and Mo
514 accumulation (Figures 4 to 7). *Os-HKT1;5* is a known Na transporter involved in rice salt
515 tolerance (Ren et al., 2005; Cotsaftis et al., 2012; Negrao et al., 2013; Platten et al., 2013).
516 However, the relationship between *Os-HKT1;5* haplotypes and Na accumulation remains
517 unclear. For example, Cotsaftis et al. (2012) suggested L395V as an essential substitution
518 affecting pore rigidity based on the 3D model of *OsHKT1;5* protein, whereas Negrao et
519 al. (2013) proposed P140A and R184H, but not L395V, as the causal alterations
520 according to their associations with salt stress tolerance. Negrao et al. (2013) genotyped
521 392 rice accessions by EcoTILLING and presented 15 haplotypes of *Os-HKT1;5*, and
522 then phenotypically characterized the most representative 59 accessions for association
523 analysis. However, due to significant difference of Na accumulations between
524 subpopulations (even between sub-subpopulations, e.g. IndI and IndII; Supplemental
525 Figure 12), comparing the ability of different haplotypes (or SNPs) across subpopulations
526 may not be appropriate. The strength of our study, compared with other previous studies,
527 lies in the large number of rice accessions within each subspecies so that the effects of
528 population structure can be excluded, and the reproducibility of the haplotype differences
529 across different sites, years and conditions. Based on analysis of data from five field
530 trials in each subpopulation, our results showed that neither L395V nor P140A had a
531 consistent effect on Na concentration (Figure 5), suggesting that they probably have no
532 or a weak function in Na variation. In contrast, we found that H184R is a key substitution
533 separating strong and weak alleles of *Os-HKT1;5* and the weak alleles are present in
534 almost all *japonica* and most *indica* accessions (Figures 4 and 5).

535 The second GWAS locus for which the causal gene was identified in our study is

536 *Os-MOT1;1*. This is the first gene identified in rice that controls Mo accumulation.
537 Different from *Os-HKT1;5* that affects Na accumulation via coding region variation, we
538 found that the variation in Mo accumulation in rice is caused by the expression levels of
539 *Os-MOT1;1* (Figures 6 and 7). This finding is similar to *MOT1;1* in *A. thaliana* (Baxter
540 et al., 2008). Further efforts will be needed to identify the causal SNPs/INDELS resulting
541 in expression level variation of *Os-MOT1;1* in promoter region.

542 In addition to *Os-HKT1;5* and *Os-MOT1;1*, we have identified candidate genes for a
543 number of loci controlling the concentrations of each of the 17 elements determined in
544 rice (Supplemental Data set 7). For example, *OsNRAMP5*, encoding a major Mn
545 transporter in rice (Sasaki et al., 2012; Yang et al., 2014), was scanned for Mn
546 concentrations at both Wuhan and Youxian locations (Supplemental Figure 20). Similarly,
547 *OsNRAMP5* has been identified by QTL mapping recently which contributes to Mn
548 variation among rice accessions via variation in the expression level (Liu et al., 2017).
549 Further investigations are needed to verify these candidate genes. Various approaches
550 including expressing genes in yeast mutants, knocking-out and overexpressing
551 candidates, or developing platform of gene expression variations by RNA sequencing can
552 be used to pick and validate candidate genes in future work. It is also noteworthy that for
553 most elements, repeated loci responsible for the same element are closely located on the
554 same chromosome (Figure 3, Supplemental Data sets 2 to 4). These close loci should be
555 considered together to aid validation of candidate genes.

556 *Indica* and *japonica* are two major subspecies in cultivated rice and have a large
557 genetic differentiation, resulting in a variety of phenotypic differences (Huang et al.,
558 2012b). In this study, we found that the large diversity was also reflected in the ionic
559 phenotypes with *japonica* accessions generally accumulating higher levels of most
560 elements than *indica* accessions (opposite pattern for Cd; Supplemental Tables 3 and 6).
561 Interestingly, we found that the GWAS loci for the same mineral element were mostly
562 not co-localized in the subpopulations of *indica* and *japonica* (Supplemental Data sets 2

563 to 4), indicating different genetic components underlying the variations of ionic traits
564 between these two subspecies. This speculation is supported by the characteristics of the
565 genes that control the variations of the rice ionome in our study. For example, the strong
566 haplotype (or Hap2) of Os-HKT1;5 existed only in *indica* but was extremely rare in the
567 *japonica* subpopulation. Os-MOT1;1 was specifically scanned in *indica* GWAS panels as
568 a possible reason of much lower Mo concentration in *indica* accessions (Supplemental
569 Figure 8). In both cases, *indica* subspecies harbors greater allelic and/or functional
570 diversity than *japonica* subspecies. These subspecies differences suggest a great potential
571 to breed across subpopulations for better nutrient uptake or salt tolerance.

572 For a number of agronomic traits including seed size, shattering habit and flowering
573 time, and metabolic traits, locations of QTLs have been shown to be conserved across
574 rice, sorghum and maize (Paterson et al., 1995; Chen et al., 2016), suggesting a
575 convergent domestication underlying these phenotypes across cereals. Common causal or
576 candidate genes were also found controlling the variations of Na (Os-*HKT1;5*/At-*HKT1*),
577 Mo (Os-*MOT1;1*/At-*MOT1*) and Cd (Os-*HMA3*/At-*HMA3*) in rice and *A. thaliana*
578 (Supplemental Data set 9) (Ueno et al., 2010; Chao et al., 2012), suggesting the
579 conservation of genetic variation at specific loci across monocots and dicots. Moreover,
580 Tm-HKT1;5-A in wheat (Munns et al., 2012), Zm-MOT1 (an ortholog of MOT1s) in
581 maize (Asaro et al., 2016), and Tc-HMA3 in *Thlaspi caerulescens* (now *Noccaea*
582 *caerulescens*) were also responsible for controlling variations of Na, Mo and Cd
583 accumulation, respectively (Ueno et al., 2011). However, the functional SNPs/INDELs
584 within each ortholog group were always different. For example, a 53 bp deletion 27
585 nucleotides upstream from the translation start site of At-MOT1 was suggested to be
586 responsible for controlling the variation of expression and the shoot Mo concentration in
587 *Arabidopsis* (Baxter et al., 2008), but this deletion was not found in the promoter region
588 of Os-MOT1;1 in rice, suggesting that other polymorphisms control the expressional
589 variation in rice (Supplemental Figure 15). Such difference suggests that the variations in

590 these loci were independently obtained by different plant species during their
591 evolutionary selection, which cause similar ionic consequences. It is unclear why
592 selection was acting on the same genes across species, but such conservation provides a
593 useful pathway to combine the discoveries of ionic loci from different plant species
594 and help mine candidate genes. It also means that the ionic GWAS loci in rice
595 identified in the present study can serve as a useful resource for other crop species.

596 *Ghd7* is an important regulator of heading date, plant height and grain yield, and
597 contributes to the variations of these traits in rice germplasm collections (Xue et al., 2008;
598 Weng et al., 2014; Zhang et al., 2015). In this study, we have identified *Ghd7* as the
599 causal gene for variations in the N concentrations in both shoots and straws (Figures 8
600 and 9). Interestingly, *Ghd7* has also been observed in a QTL related to N-deficiency
601 tolerance in rice (Wei et al., 2012). Here we found that N concentration in rice collections
602 was highly correlated with heading date (Supplemental Figure 17), and overexpressing a
603 functional allele of *Ghd7* in rice plants significantly decreased N accumulation (Figure 8).
604 A recent research showed that the enhanced expression of *Ghd7* lowered the chlorophyll
605 content (Wang et al., 2015), which could be explained by the negative effect of *Ghd7* on
606 N concentration observed in our study. Another important gene for rice yield, *DEP1*, has
607 recently been shown to regulate nitrogen-use efficiency in rice (Sun et al., 2014).
608 Mutation of *DEP1* resulted in decreased plant height and increased N concentration, but
609 did not affect heading date. We suggest that these key genes of agronomic traits and
610 nitrogen form a complex relationship in regulating plant growth and N accumulation. In
611 our collection, we found significant negative correlation between biomass and N
612 concentrations at both the heading and mature stages, but significant positive correlation
613 between biomass and the total amount of N accumulated (Supplemental Figure 19).
614 These opposite relationships suggest both that cultivars with higher biomass are able to
615 acquire more N from the soil and that there is a dilution effect of increasing biomass on
616 the N concentration. It is therefore important to identify loci that are associated together

617 with biomass, grain yield and N concentrations (Supplemental Table 7). These loci would
618 provide more chances to investigate the relationship between N concentrations with
619 biomass as well as grain yield, and also would benefit breeding rice with high
620 nitrogen-use efficiency as well as high yield.

621 Reducing the inputs of N and P fertilizers while maintaining high yield and quality is
622 crucial for agricultural sustainability. Crop breeding is an important tool for realizing this
623 goal. The present study has shown that N and P deficiencies can affect the ionic
624 profile of rice plants, thus impacting grain quality by altering the concentrations of
625 essential and toxic elements (Supplemental Figure 1 and Supplemental Table 1).
626 Moreover, the extent of influence for different elements by nutritional status is obviously
627 different. Analyses of the genetic basis of variation in the ionic profile under different
628 N and P supply conditions reveal both the conservative and non-conservative genetic
629 components in controlling the ionic profile in response to the altered nutrient status.
630 Moreover, we have identified loci for element concentrations that are highly dependent
631 on the N or P supply (Supplemental Data set 11). Isolation of the causal genes for these
632 loci would help to unravel the complex crosstalk between N or P and other elements in
633 rice plants.

634 In conclusion, we have described a comprehensive study of the rice ionome
635 combining genetic methodologies with high-throughput elemental profiling to dissect the
636 genetic basis of variations of 17 mineral elements in rice. Our study reveals at least 72
637 common locus-element associations showing high reproducibility under different field
638 conditions and a large number of specific loci corresponding to different field conditions.
639 We have identified strong candidates for three of the loci, including the first evidence that
640 *Os-MOT1;1* is involved in the variation of Mo accumulation and the effect of heading
641 date gene *Ghd7* on N concentration in rice. The information of the locus-element
642 associations obtained in the present study provides an important foundation for future
643 studies on the genetic and molecular mechanisms controlling the rice ionome.

644

645 **Methods**

646 **Plant Materials and Sequencing Data.**

647 A set of 529 rice accessions was collected and sequenced as described previously (Chen
648 et al., 2014). The set included 192 accessions from a core/minicore collection of *O.*
649 *sativa* L. in China (Zhang et al., 2011), 132 parental lines used in the International Rice
650 Molecular Breeding Program (Yu et al., 2003), 148 accessions from a minicore subset of
651 the US Department of Agriculture rice gene bank (Agrama et al., 2009), 15 accessions
652 used for SNP discovery in the OryzaSNP project (McNally et al., 2009), and 46
653 additional accessions from the Rice Germplasm Center at the IRRI. Information about
654 the accessions, including names, countries of origin, geographical locations, and
655 subpopulation classification, is listed in Supplemental Data set 1. We sequenced the 529
656 accessions using the Illumina HiSeq 2000 in the form of 90-bp paired-end reads to
657 generate high-quality sequences of more than 1 Gb per accession (>2.5× per genome,
658 total 6.7 billion reads). These raw data are available in NCBI with BioProject accession
659 number PRJNA171289. The assembly release version 6.1 of genomic pseudomolecules
660 of *japonica* cv. Nipponbare, downloaded from the rice annotation database of Michigan
661 State University (MSU), was used as the reference genome. We performed imputation by
662 using an in-house modified k nearest neighbour algorithm. The detailed procedures of
663 data analysis have been described in our previous articles (Chen et al., 2014; Xie et al.,
664 2015). The SNP information is available on the RiceVarMap website (Zhao et al., 2014).
665 The wild-type, mutant and transgenic plants related to Os-MOT1;1 used in the present
666 study were all based on the background of the cv. Zhonghua 11 (*O. sativa* L. ssp.
667 *japonica* variety). The *osmot1;1* mutant is a T-DNA insertion mutant (ID: 03Z11DK23)
668 identified from the Rice Mutant Database (Wu et al., 2003; Zhang et al., 2006).

669

670 **Field trials and Sample preparation**

671 Field trials were conducted at two locations in China, including the experimental farm of
672 Huazhong Agricultural University in Wuhan, Hubei province, and an experimental farm
673 in Youxian, Hunan province. At Wuhan, the seeds of 529 rice accessions were
674 germinated in a seed bed in mid May 2012 and were transplanted to three adjacent paddy
675 fields with different nutritional status in mid-June 2012. The three different fields,
676 including a normal field (NF) receiving standard fertilizer inputs, a low nitrogen field
677 (LN) and a low phosphate field (LP), were constructed by controlling fertilizer
678 applications in the recent decade. Fertilizers were applied (per hectare) as follows: 90 kg
679 N, 45 kg P, and 72 kg K in the NF field; 45 kg P, and 72 kg K in the LN field; 90 kg N
680 and 72 kg K in the LP field. At Youxian, the field trials were performed for two
681 consecutive years (2014 and 2015). The seeds of 529 rice accessions were germinated in
682 mid-May and the Seedlings about 25 days old were transplanted to the field in each year.
683 Before rice transplanting, we randomly collected 11~13 soil samples in each field for the
684 analyses of soil nutrient (and heavy metals/metalloids/pH values) status (Supplemental
685 Tables 4). The irrigation water was also analyzed (Supplemental Tables 8). Each
686 accession was planted in two replicates in each field at Wuhan and planted in three
687 replicates for each year at Youxian, with 20 plants (two rows of ten plants) in each
688 replicate, in a randomized complete block design. The planting density was 16.5 cm
689 between plants in a row and 26 cm between rows. The trials were managed according to
690 normal agricultural practices with regards to crop protection and paddy water
691 management (considering the varied heading dates in different accessions, we drained the
692 paddy water in early September for about 15 days, and then irrigated again for about a
693 week, and drained the water in late September). Five plants of each accession were
694 harvested at the heading stage, and another five plants were harvested at the maturity
695 stage (40 days after flowering for each line). All plants taken for analysis were the ones
696 in the inside lines. The five plants were combined to represent one biological replicate.
697 Plant samples at maturity were separated into straw and brown rice (dehusked).

698

699 **Elemental analysis**

700 Plant samples were dried at 80 °C for 3 d and ground to fine powders. For the
701 determinations of N and P concentrations, 0.2 g dried powder was digested with 5 ml of
702 98% H₂SO₄ and 5 ml of 30% hydrogen peroxide. After cooling, the digested sample was
703 diluted to 100 ml with distilled water. The N concentration in the solution was
704 determined colourimetrically at 660 nm using a modified Berthelot reaction with
705 salicylate, dichloroisocyanurate and complex cyanides on an automated discrete analyser
706 (SmartChem 200, France). The P concentration in the solution was measured using the
707 molybdate blue method with absorbance read at 880 nm on an automated discrete
708 analyser. For the determinations of other mineral elements, 0.2 g dried powder of each
709 sample was digested in 65% nitric acid in a MARS6 microwave (CEM) with a gradient
710 of temperatures from 120 °C to 180 °C for 45min. After dilution in deionized water, the
711 concentrations of 15 elements determined by inductively coupled plasma mass
712 spectrometry (ICP-MS, Agilent 7700 series, USA).

713

714 **Genome-Wide Association Analyses**

715 SNPs with minor allele frequency ≥ 0.05 and the number of rice accessions with the
716 minor allele ≥ 15 in the population were used to carry out GWAS. In total, 2,767,191 and
717 1,857,866 SNPs were used in GWAS for subpopulations of *indica* and *japonica*,
718 respectively. To control spurious associations, population structure was modeled as a
719 random effect in LMM using the kinship (K) matrix. The evenly distributed random SNP
720 set used to analyze population structure was used to calculate K. GWAS was performed
721 by using LMM and LR provided by the FaST-LMM program. According to a modified
722 Bonferroni correction described by Li et al. (Li et al., 2012), the effective number of
723 independent SNPs (Me) in each population was calculated and then used to replace the
724 total number of SNPs to determine the genome-wide significance thresholds of the

725 GWAS. The Me was calculated as 571,843 and 245,348 for the subpopulations of *indica*
726 and *japonica*, respectively, and the suggestive *P* values were specified as 1.8×10^{-6} in
727 *indica* and 4.1×10^{-6} in *japonica*. The corresponding thresholds were then set to identify
728 significant association signals by LMM. To obtain independent association signals,
729 multiple SNPs exceeding the threshold in a 5-Mb region were clustered by r^2 of LD \geq
730 0.25, and SNPs with the lowest *P*-value in a cluster were considered as lead SNPs. The
731 detailed method has been described in previous studies (Chen et al., 2014).

732

733 **Vector construction and rice transformation**

734 To generate the overexpression constructs of *Os-MOT1;1*, four types (Type 1 – 4) of full
735 length cDNA of *Os-MOT1;1* were amplified by using primers
736 *Os-MOT1;1-OX-F/Os-MOT1;1-OX-R* from four different rice accessions: W024, W102,
737 C020 and C055, respectively. The amplified cDNA was first introduced into the gateway
738 vector pDONR207 and then transferred into the destination vector pJC034 using the
739 Gateway recombination reaction (Invitrogen). The constructs were transformed into cv.
740 Zhonghua 11 by *Agrobacterium tumefaciens*-mediated transformation. To construct the
741 *MOT1;1-promoter:GUS* plasmid, 2.5 kb of genomic sequence located upstream of the
742 *Os-MOT1;1* initiation codon was amplified by using primers
743 *Os-MOT1;1-P-F/Os-MOT1;1-P-R* from cv. Nipponbare genomic DNA. The amplified
744 promoter fragment was then cloned into pDONR207 and then transformed into the
745 Gateway-compatible GUS fusion vector pGWB3 by Gateway recombination reaction. Cv.
746 Zhonghua 11 calli was transformed with this construct. The transgenic plant tissues were
747 incubated in an X-Gluc staining buffer at 37 °C for 4 h. To generate the overexpression
748 constructs of *Ghd7*, the full length cDNA of a functional allele of *Ghd7* was amplified by
749 using primers *Ghd7-OX-F/Ghd7-OX-R* from Cv. Minghui 63. The amplified cDNA was
750 first introduced into the pGEM-T vector (Promega) and then cloned into a modified
751 overexpression vector PU1301^{GPF} with *Xho*I and *Bam*HI sites. All the primers used for

752 vector constructions were listed in Supplemental Table 9.

753

754 **Hydroponic experiments**

755 For expression analysis of *Os-MOT1;1* and the determination of Mo concentrations in
756 roots and shoots of both transgenic and wild-type plants, hydroponic experiments were
757 performed according the standard rice culture solution (1.44 mM NH₄NO₃, 0.3 mM
758 NaH₂PO₄, 0.5 mM K₂SO₄, 1.0 mM CaCl₂, 1.6 mM MgSO₄, 0.17 mM Na₂SiO₃, 50 μM
759 Fe-EDTA, 0.06 μM (NH₄)₆Mo₇O₂₄, 15 μM H₃BO₃, 8 μM MnCl₂, 0.12 μM CuSO₄, 0.12
760 μM ZnSO₄, 29 μM FeCl₃ and 40.5 μM citric acid and adjust pH to 5.5 by sulfuric
761 acid)(Yoshida et al., 1976). Rice plants were grown in full nutrient solution or Mo
762 deficiency solution (full nutrient solution without Mo) for about four weeks after
763 germination. The nutrient solution was renewed every 5 days. For both expressional and
764 elemental analysis, three plants (or tissues from three different plants) were mixed in one
765 replication, and three biological replicates were conducted for each line.

766

767 **RNA extraction and real-time PCR**

768 Total RNA was extracted using Trizol reagent (Invitrogen). The first-strand cDNAs were
769 synthesized with 3 μg of total RNA in 20 μl of reaction mixture by using SuperScript III
770 reverse transcriptase (Invitrogen) according to the manufacturer's instructions. Real-time
771 PCR was performed by using the SYBR Premix Ex Taq™ (TaKaRa) on an Applied
772 Biosystems 7500 PCR instrument. The rice Ubiquitin5 gene was used as the internal
773 control with primers qUbq-F/qUbq-R. The expression measurements were made by using
774 the relative quantification method (Livak and Schmittgen, 2001). All the primers used for
775 real-time PCR were listed in Supplemental Table 9.

776

777 **Statistical analyses**

778 Broad-sense heritability (H^2) was calculated using the following equation by treating

779 accessions as a random effect and the biological replication as a replication effect using
780 one-way analysis of variance (ANOVA) as described previously (Chen et al., 2014): $H^2 =$
781 $\text{var}_{(G)}/(\text{var}_{(G)} + \text{var}_{(E)})$, where $\text{var}_{(G)}$ and $\text{var}_{(E)}$ are the variance derived from genetic and
782 environmental effects, respectively. LD was estimated by using standardized
783 disequilibrium coefficients (D'), and squared allele-frequency correlations (r^2) for pairs
784 of SNP loci were determined according to the TASSEL program (Bradbury et al., 2007).
785 LD plots were generated in Haploview (Barrett, 2009), indicating r^2 values between pairs
786 of SNPs multiplied by 100 and color coded with white ($r^2 = 0$), shades of gray ($0 < r^2 < 1$)
787 and black ($r^2 = 1$).

788

789 **Accession Numbers**

790 Sequence data used in this article can be found in the GenBank/EMBL database under
791 the following accession numbers: Os-HKT1;5 (Os01g0307500), Os-MOT1;1
792 (Os08g0101500), and Ghd7 (Os07g0261200).

793

794 **Supplemental Data**

795 **Supplemental Figure 1.** Box plots for elemental concentrations among different field
796 conditions at Wuhan.

797 **Supplemental Figure 2.** Principal component analysis of ionome between normal and
798 low fertilizer field conditions.

799 **Supplemental Figure 3.** Hierarchical clustering of natural accessions based on their
800 ionome.

801 **Supplemental Figure 4.** Box plots for elemental concentrations at Wuhan field
802 conditions.

803 **Supplemental Figure 5.** Box plots for elemental concentrations at Youxian field
804 conditions.

805 **Supplemental Figure 6.** Box plots for concentrations of some elements at Wuhan field

806 conditions after the Box–Cox transformation.

807 **Supplemental Figure 7.** Box plots for concentrations of some elements at Youxian field
808 conditions after the Box–Cox transformation.

809 **Supplemental Figure 8.** A presentation of some Manhattan and Q-Q plots which
810 showed relatively well repeatability and significance for these elements.

811 **Supplemental Figure 9.** A presentation of local linkage disequilibrium for a few loci in
812 corresponding diversity panels.

813 **Supplemental Figure 10.** A list for all haplotypes of Os-HKT1;5 in 1479 or 529 natural
814 accessions.

815 **Supplemental Figure 11.** Geographical distribution of the accessions possessing
816 different haplotypes of Os-HKT1;5 on part of the world map.

817 **Supplemental Figure 12.** Analysis of Na concentrations in different subgroups within
818 each Os-HKT1;5 haplotype in our collection.

819 **Supplemental Figure 13.** Histochemical staining of GUS activity in rice plants
820 transformed with the Os-*MOT1;1*-promoter:*GUS* construct.

821 **Supplemental Figure 14.** Identification of the T-DNA inserted line of Os-*MOT1;1*.

822 **Supplemental Figure 15.** Sequence alignment of Os-*MOT1;1* promoter region in *indica*
823 subpopulation based on fully sequencing data of 20 *indica* accessions.

824 **Supplemental Figure 16.** Sequence alignment of Os-*MOT1;1* CDS in *indica*
825 subpopulation based on fully sequencing data of 20 *indica* accessions.

826 **Supplemental Figure 17** The correlation between heading date and iomome at Wuhan
827 revealed by a heat map of correlation coefficient.

828 **Supplemental Figure 18.** Box plots for grain yield and biomass of natural population of
829 cultivated rice at three different field conditions of Wuhan location.

830 **Supplemental Figure 19.** Correlation among N concentrations, biomass and grain yield
831 in natural population of cultivated rice at Wuhan location.

832 **Supplemental Figure 20.** Characterization of Os-NRAMP5 by GWAS.

833 **Supplemental Table 1.** Means and standard deviations of elemental concentrations of
834 natural population of cultivated rice in each tissue and at each field of Wuhan location.

835 **Supplemental Table 2.** The broad-sense heritability (H^2) for each element across two
836 biological replicates at Wuhan location.

837 **Supplemental Table 3.** The overall ratio of elemental concentrations between *indica* and
838 *japonica* at location of Wuhan.

839 **Supplemental Table 4.** Soil nutrient status.

840 **Supplemental Table 5.** The broad-sense heritability (H^2) for each element across two
841 consecutive years at Youxian location.

842 **Supplemental Table 6.** The overall ratio of elemental concentrations between *indica* and
843 *japonica* at location of Youxian.

844 **Supplemental Table 7.** Co-localized GWAS loci among traits of above-ground biomass
845 at heading stage, above-ground biomass at maturation stage and grain yield.

846 **Supplemental Table 8.** Elemental analysis in irrigation water.

847 **Supplemental Table 9.** Primers used in this study.

848 **Supplemental Data set 1.** Information of 529 accessions used in this study.

849 **Supplemental Data set 2.** The information of 41 common loci which were repeatedly
850 scanned in at least two field conditions at Wuhan.

851 **Supplemental Data set 3.** The information of 14 common loci which were repeatedly
852 scanned in two consecutive years at Youxian.

853 **Supplemental Data set 4.** The information of 32 common loci which were repeatedly
854 scanned across locations of Wuhan and Youxian.

855 **Supplemental Data set 5.** Co-localization of the 72 common loci (from **Supplemental**
856 **Data set 2, 3 and 4** after remove duplicates) with the previously detected element-related
857 QTLs in rice.

858 **Supplemental Data set 6.** Gene list within 300 kb of the all 72 common loci which were
859 repeatedly scanned at Wuhan or Youxian for 17 elements.

860 **Supplemental Data set 7.** Potential candidate genes (or known element-related genes) in
861 the 72 loci which were repeatedly scanned for 17 elements.

862 **Supplemental Data set 8.** Ionomics GWAS data in *A. thaliana* based on leaf ionomic
863 data of ~349 accessions.

864 **Supplemental Data set 9.** List of orthologous genes obtained by comparing ionomic
865 GWAS data between rice and *A. thaliana*.

866 **Supplemental Data set 10.** The heading dates of 529 accessions used in this study when
867 cultivated in Wuhan, China, and the Ghd7 haplotype for each accession based on its
868 SNPs information.

869 **Supplemental Data set 11.** List of the loci which were scanned across tissues at Wuhan.

870

871 **ACKNOWLEDGMENTS**

872 This work was supported by grants from the National Natural Science Foundation of
873 China (numbers 31520103914 and 31471932), the National High Technology Research
874 and Development Program of China (number 2014AA10A603) and the Special Fund for
875 Agro-scientific Research in the Public Interest (number 201403015).

876

877 **AUTHOR CONTRIBUTIONS**

878 X. L. conceived the project and supervised the study. M.Y., K.L., G.Y., Q.D., C.S., L.L.,
879 H.D., and J.H. performed the experiments. M.Y., K.L., F.J.Z., W.X., P.R., H.Z., X.Y.H.
880 and L.M. analyzed the data. M.Y., W.X., H.Z., Z.Z., W.W., Y.X., G.W., J.X. and X.L.
881 contributed reagents/materials/analysis tools. M.Y., F.J.Z. X.Y.H., D.E.S. and X.L. wrote
882 the paper. All of the authors discussed the results and commented on the manuscript.

883

884 **COMPETING FINANCIAL INTERESTS**

885 The authors declare no competing financial interests.

886

887

888 **Reference**

- 889 **Agrama, H.A., Yan, W.G., Lee, F., Fjellstrom, R., Chen, M.H., Jia, M., and McClung, A.** (2009).
890 Genetic Assessment of a Mini-Core Subset Developed from the USDA Rice Genebank. *Crop Sci.* **49**,
891 1336-1346.
- 892 **Arao, T., and Ae, N.** (2003). Genotypic variations in cadmium levels of rice grain. *Soil Sci. Plant Nutr.* **49**,
893 473-479.
- 894 **Asaro, A., Ziegler, G., Ziyomo, C., Hoekenga, O.A., Dilkes, B.P., and Baxter, I.** (2016). The Interaction
895 of Genotype and Environment Determines Variation in the Maize Kernel Ionome. *G3* (Bethesda, Md.)
896 **6**, 4175-4183.
- 897 **Axelsen, K.B., and Palmgren, M.G.** (2001). Inventory of the superfamily of P-type ion pumps in
898 *Arabidopsis*. *Plant Physiol.* **126**, 696-706.
- 899 **Barrett, J.C.** (2009). Haploview: Visualization and analysis of SNP genotype data. *Cold Spring Harb*
900 *Protoc* **2009**, pdb ip71.
- 901 **Baxter, I., Hermans, C., Lahner, B., Yakubova, E., Tikhonova, M., Verbruggen, N., Chao, D.Y., and**
902 **Salt, D.E.** (2012). Biodiversity of mineral nutrient and trace element accumulation in *Arabidopsis*
903 *thaliana*. *PLoS One* **7**, e35121.
- 904 **Baxter, I., Muthukumar, B., Park, H.C., Buchner, P., Lahner, B., Danku, J., Zhao, K., Lee, J.,**
905 **Hawkesford, M.J., Guerinot, M.L., and Salt, D.E.** (2008). Variation in molybdenum content across
906 broadly distributed populations of *Arabidopsis thaliana* is controlled by a mitochondrial molybdenum
907 transporter (MOT1;1). *PLoS Genet.* **4**, e1000004.
- 908 **Baxter, I., Brazelton, J.N., Yu, D., Huang, Y.S., Lahner, B., Yakubova, E., Li, Y., Bergelson, J.,**
909 **Borevitz, J.O., Nordborg, M., Vitek, O., and Salt, D.E.** (2010). A coastal cline in sodium
910 accumulation in *Arabidopsis thaliana* is driven by natural variation of the sodium transporter
911 AtHKT1;1. *PLoS Genet.* **6**, e1001193.
- 912 **Bradbury, P.J., Zhang, Z., Kroon, D.E., Casstevens, T.M., Ramdoss, Y., and Buckler, E.S.** (2007).
913 TASSEL: software for association mapping of complex traits in diverse samples. *Bioinformatics* **23**,
914 2633-2635.
- 915 **Chao, D.Y., Silva, A., Baxter, I., Huang, Y.S., Nordborg, M., Danku, J., Lahner, B., Yakubova, E., and**
916 **Salt, D.E.** (2012). Genome-Wide Association Studies Identify Heavy Metal ATPase3 as the Primary
917 Determinant of Natural Variation in Leaf Cadmium in *Arabidopsis thaliana*. *PLoS Genet.* **8**.
- 918 **Chao, D.Y., Chen, Y., Chen, J., Shi, S., Chen, Z., Wang, C., Danku, J.M., Zhao, F.J., and Salt, D.E.**
919 (2014). Genome-wide association mapping identifies a new arsenate reductase enzyme critical for
920 limiting arsenic accumulation in plants. *PLoS Biol.* **12**, e1002009.
- 921 **Chen, H., Tang, Z., Wang, P., and Zhao, F.J.** (2018). Geographical variations of cadmium and arsenic
922 concentrations and arsenic speciation in Chinese rice. *Environ. Pollut.* **238**, 482-490.
- 923 **Chen, W., et al.** (2014). Genome-wide association analyses provide genetic and biochemical insights into
924 natural variation in rice metabolism. *Nat. Genet.* **46**, 714-721.
- 925 **Chen, W., Wang, W., Peng, M., Gong, L., Gao, Y., Wan, J., Wang, S., Shi, L., Zhou, B., Li, Z., Peng,**
926 **X., Yang, C., Qu, L., Liu, X., and Luo, J.** (2016). Comparative and parallel genome-wide association

927 studies for metabolic and agronomic traits in cereals. *Nat Commun* **7**, 12767.

928 **Clemens, S., and Ma, J.F.** (2016). Toxic Heavy Metal and Metalloid Accumulation in Crop Plants and
929 Foods. *Annu. Rev. Plant Biol.* **67**, 489-512.

930 **Clemens, S., Palmgren, M.G., and Kramer, U.** (2002). A long way ahead: understanding and engineering
931 plant metal accumulation. *Trends Plant Sci.* **7**, 309-315.

932 **Cotsaftis, O., Plett, D., Shirley, N., Tester, M., and Hrmova, M.** (2012). A two-staged model of Na⁺
933 exclusion in rice explained by 3D modeling of HKT transporters and alternative splicing. *PLoS One* **7**,
934 e39865.

935 **Du, J., Zeng, D., Wang, B., Qian, Q., Zheng, S., and Ling, H.Q.** (2013). Environmental effects on
936 mineral accumulation in rice grains and identification of ecological specific QTLs. *Environ. Geochem.*
937 *Health* **35**, 161-170.

938 **Duan, G.L., Shao, G.S., Tang, Z., Chen, H.P., Wang, B.X., Tang, Z., Yang, Y.P., Liu, Y.C., and Zhao,**
939 **F.J.** (2017). Genotypic and Environmental Variations in Grain Cadmium and Arsenic Concentrations
940 Among a Panel of High Yielding Rice Cultivars. *Rice* **10**.

941 **Famoso, A.N., Zhao, K., Clark, R.T., Tung, C.W., Wright, M.H., Bustamante, C., Kochian, L.V., and**
942 **McCouch, S.R.** (2011). Genetic Architecture of Aluminum Tolerance in Rice (*Oryza sativa*)
943 Determined through Genome-Wide Association Analysis and QTL Mapping. *PLoS Genet.* **7**.

944 **Forsberg, S.K., Andreatta, M.E., Huang, X.Y., Danku, J., Salt, D.E., and Carlborg, O.** (2015). The
945 Multi-allelic Genetic Architecture of a Variance-Heterogeneity Locus for Molybdenum Concentration
946 in Leaves Acts as a Source of Unexplained Additive Genetic Variance. *PLoS Genet.* **11**, e1005648.

947 **Garcia-Oliveira, A.L., Tan, L., Fu, Y., and Sun, C.** (2009). Genetic identification of quantitative trait loci
948 for contents of mineral nutrients in rice grain. *J. Integr. Plant Biol.* **51**, 84-92.

949 **Hermans, C., Hammond, J.P., White, P.J., and Verbruggen, N.** (2006). How do plants respond to
950 nutrient shortage by biomass allocation? *Trends Plant Sci.* **11**, 610-617.

951 **Hirel, B., Le Gouis, J., Ney, B., and Gallais, A.** (2007). The challenge of improving nitrogen use
952 efficiency in crop plants: towards a more central role for genetic variability and quantitative genetics
953 within integrated approaches. *J. Exp. Bot.* **58**, 2369-2387.

954 **Horie, T., Hauser, F., and Schroeder, J.I.** (2009). HKT transporter-mediated salinity resistance
955 mechanisms in *Arabidopsis* and monocot crop plants. *Trends Plant Sci.* **14**, 660-668.

956 **Hu, B., et al.** (2015). Variation in NRT1.1B contributes to nitrate-use divergence between rice subspecies.
957 *Nat. Genet.*

958 **Huang, X., et al.** (2012a). Genome-wide association study of flowering time and grain yield traits in a
959 worldwide collection of rice germplasm. *Nat. Genet.* **44**, 32-39.

960 **Huang, X., et al.** (2012b). A map of rice genome variation reveals the origin of cultivated rice. *Nature* **490**,
961 497-501.

962 **Huang, X.H., and Han, B.** (2014). Natural Variations and Genome-Wide Association Studies in Crop
963 Plants. *Annu. Rev. Plant Biol.* **65**, 531-551.

964 **Huang, X.H., et al.** (2010). Genome-wide association studies of 14 agronomic traits in rice landraces. *Nat.*
965 *Genet.* **42**, 961-U976.

966 **Huang, X.Y., and Salt, D.E.** (2016). Plant Ionomics: From Elemental Profiling to Environmental
967 Adaptation. *Mol Plant* **9**, 787-797.

968 **Huang, X.Y., Deng, F., Yamaji, N., Pinson, S.R., Fujii-Kashino, M., Danku, J., Douglas, A., Guerinot,**
969 **M.L., Salt, D.E., and Ma, J.F.** (2016). A heavy metal P-type ATPase OsHMA4 prevents copper
970 accumulation in rice grain. *Nat Commun* **7**, 12138.

971 **Jiao, Y., Wang, Y., Xue, D., Wang, J., Yan, M., Liu, G., Dong, G., Zeng, D., Lu, Z., Zhu, X., Qian, Q.,**
972 **and Li, J.** (2010). Regulation of OsSPL14 by OsmiR156 defines ideal plant architecture in rice. *Nat.*
973 *Genet.* **42**, 541-544.

974 **Jung, C., and Muller, A.E.** (2009). Flowering time control and applications in plant breeding. *Trends*
975 *Plant Sci.* **14**, 563-573.

976 **Lahner, B., Gong, J.M., Mahmoudian, M., Smith, E.L., Abid, K.B., Rogers, E.E., Guerinot, M.L.,**
977 **Harper, J.F., Ward, J.M., McIntyre, L., Schroeder, J.I., and Salt, D.E.** (2003). Genomic scale
978 profiling of nutrient and trace elements in *Arabidopsis thaliana*. *Nat. Biotechnol.* **21**, 1215-1221.

979 **Li, M.X., Yeung, J.M., Cherny, S.S., and Sham, P.C.** (2012). Evaluating the effective numbers of
980 independent tests and significant *p*-value thresholds in commercial genotyping arrays and public
981 imputation reference datasets. *Hum. Genet.* **131**, 747-756.

982 **Liu, C., Chen, G., Li, Y., Peng, Y., Zhang, A., Hong, K., Jiang, H., Ruan, B., Zhang, B., Yang, S., Gao,**
983 **Z., and Qian, Q.** (2017). Characterization of a major QTL for manganese accumulation in rice grain.
984 *Sci. Rep.* **7**, 17704.

985 **Livak, K.J., and Schmittgen, T.D.** (2001). Analysis of relative gene expression data using real-time
986 quantitative PCR and the 2(-Delta Delta C(T)) Method. *Methods* **25**, 402-408.

987 **Lu, K.Y., Li, L.Z., Zheng, X.F., Zhang, Z.H., Mou, T.M., and Hu, Z.L.** (2008). Quantitative trait loci
988 controlling Cu, Ca, Zn, Mn and Fe content in rice grains. *J Genet* **87**, 305-310.

989 **Lu, L., Yan, W., Xue, W., Shao, D., and Xing, Y.** (2012). Evolution and association analysis of Ghd7 in
990 rice. *PLoS One* **7**, e34021.

991 **Mahender, A., Anandan, A., Pradhan, S.K., and Pandit, E.** (2016). Rice grain nutritional traits and their
992 enhancement using relevant genes and QTLs through advanced approaches. *Springerplus* **5**.

993 **Marschner, H., and Marschner, P.** (2012). *Marschner's mineral nutrition of higher plants.* (London ;
994 Waltham, MA: Elsevier/Academic Press).

995 **Matsuda, F., Nakabayashi, R., Yang, Z., Okazaki, Y., Yonemaru, J., Ebana, K., Yano, M., and Saito,**
996 **K.** (2015). Metabolome-genome-wide association study dissects genetic architecture for generating
997 natural variation in rice secondary metabolism. *Plant J.* **81**, 13-23.

998 **Matsumoto, T., et al.** (2005). The map-based sequence of the rice genome. *Nature* **436**, 793-800.

999 **McNally, K.L., et al.** (2009). Genomewide SNP variation reveals relationships among landraces and
1000 modern varieties of rice. *Proc. Natl. Acad. Sci. U. S. A.* **106**, 12273-12278.

1001 **Ming, R., Del Monte, T.A., Hernandez, E., Moore, P.H., Irvine, J.E., and Paterson, A.H.** (2002).
1002 Comparative analysis of QTLs affecting plant height and flowering among closely-related diploid and
1003 polyploid genomes. *Genome* **45**, 794-803.

1004 **Miyadate, H., Adachi, S., Hiraizumi, A., Tezuka, K., Nakazawa, N., Kawamoto, T., Katou, K.,**
1005 **Kodama, I., Sakurai, K., Takahashi, H., Satoh-Nagasawa, N., Watanabe, A., Fujimura, T., and**
1006 **Akagi, H.** (2011). OsHMA3, a P-1B-type of ATPase affects root-to-shoot cadmium translocation in
1007 rice by mediating efflux into vacuoles. *New Phytol.* **189**, 190-199.

1008 **Morrissey, J., Baxter, I.R., Lee, J., Li, L.T., Lahner, B., Grotz, N., Kaplan, J., Salt, D.E., and**

1009 **Guerinot, M.L.** (2009). The Ferroportin Metal Efflux Proteins Function in Iron and Cobalt
1010 Homeostasis in *Arabidopsis*. *Plant Cell* **21**, 3326-3338.

1011 **Munns, R., James, R.A., Xu, B., Athman, A., Conn, S.J., Jordans, C., Byrt, C.S., Hare, R.A.,**
1012 **Tyerman, S.D., Tester, M., Plett, D., and Gilliham, M.** (2012). Wheat grain yield on saline soils is
1013 improved by an ancestral Na⁺ transporter gene. *Nat. Biotechnol.* **30**, 360-U173.

1014 **Nawaz, Z., Kakar, K.U., Li, X.B., Li, S., Zhang, B., Shou, H.X., and Shu, Q.Y.** (2015). Genome-wide
1015 Association Mapping of Quantitative Trait Loci (QTLs) for Contents of Eight Elements in Brown Rice
1016 (*Oryza sativa* L.). *J. Agric. Food Chem.* **63**, 8008-8016.

1017 **Negrao, S., Almadanim, M.C., Pires, I.S., Abreu, I.A., Maroco, J., Courtois, B., Gregorio, G.B.,**
1018 **McNally, K.L., and Oliveira, M.M.** (2013). New allelic variants found in key rice salt-tolerance
1019 genes: an association study. *Plant Biotechnol. J.* **11**, 87-100.

1020 **Norton, G.J., Deacon, C.M., Xiong, L.Z., Huang, S.Y., Meharg, A.A., and Price, A.H.** (2010). Genetic
1021 mapping of the rice ionome in leaves and grain: identification of QTLs for 17 elements including
1022 arsenic, cadmium, iron and selenium. *Plant Soil* **329**, 139-153.

1023 **Norton, G.J., Duan, G.L., Lei, M., Zhu, Y.G., Meharg, A.A., and Price, A.H.** (2012a). Identification of
1024 quantitative trait loci for rice grain element composition on an arsenic impacted soil: Influence of
1025 flowering time on genetic loci. *Ann. Appl. Biol.* **161**, 46-56.

1026 **Norton, G.J., et al.** (2012b). Variation in grain arsenic assessed in a diverse panel of rice (*Oryza sativa*)
1027 grown in multiple sites. *New Phytol.* **193**, 650-664.

1028 **Norton, G.J., et al.** (2014). Genome Wide Association Mapping of Grain Arsenic, Copper, Molybdenum
1029 and Zinc in Rice (*Oryza sativa* L.) Grown at Four International Field Sites. *PLoS One* **9**, e89685.

1030 **Ohmori, Y., Sotta, N., and Fujiwara, T.** (2016). Identification of introgression lines of *Oryza glaberrima*
1031 Steud. with high mineral content in grains. *Soil Sci. Plant Nutr.* **62**, 456-464.

1032 **Palmgren, M.G.** (2001). PLANT PLASMA MEMBRANE H⁺-ATPases: Powerhouses for Nutrient Uptake.
1033 *Annu. Rev. Plant Physiol. Plant Mol. Biol.* **52**, 817-845.

1034 **Paterson, A.H., Lin, Y.R., Li, Z., Schertz, K.F., Doebley, J.F., Pinson, S.R., Liu, S.C., Stansel, J.W.,**
1035 **and Irvine, J.E.** (1995). Convergent domestication of cereal crops by independent mutations at
1036 corresponding genetic Loci. *Science* **269**, 1714-1718.

1037 **Platten, J.D., Egdane, J.A., and Ismail, A.M.** (2013). Salinity tolerance, Na⁺ exclusion and allele mining
1038 of HKT1;5 in *Oryza sativa* and *O. glaberrima*: many sources, many genes, one mechanism? *BMC*
1039 *Plant Biol.* **13**, 32.

1040 **Pinson, S.R.M., Tarpley, L., Yan, W.G., Yeater, K., Lahner, B., Yakubova, E., Huang, X.Y., Zhang, M.,**
1041 **Guerinot, M.L., and Salt, D.E.** (2015). Worldwide Genetic Diversity for Mineral Element
1042 Concentrations in Rice Grain. *Crop Sci.* **55**, 294-311.

1043 **Ren, Z.H., Gao, J.P., Li, L.G., Cai, X.L., Huang, W., Chao, D.Y., Zhu, M.Z., Wang, Z.Y., Luan, S.,**
1044 **and Lin, H.X.** (2005). A rice quantitative trait locus for salt tolerance encodes a sodium transporter.
1045 *Nat. Genet.* **37**, 1141-1146.

1046 **Salt, D.E., Baxter, I., and Lahner, B.** (2008). Ionomics and the study of the plant ionome. *Annual Review*
1047 *of Plant Biology*, Vol 63 **59**, 709-733.

1048 **Sasaki, A., Yamaji, N., Yokosho, K., and Ma, J.F.** (2012). Nramp5 is a major transporter responsible for
1049 manganese and cadmium uptake in rice. *Plant Cell* **24**, 2155-2167.

1050 **Segura, V., Vilhjalmsson, B.J., Platt, A., Korte, A., Seren, U., Long, Q., and Nordborg, M.** (2012). An
1051 efficient multi-locus mixed-model approach for genome-wide association studies in structured
1052 populations. *Nat. Genet.* **44**, 825-830.

1053 **Seren, U., Vilhjalmsson, B.J., Horton, M.W., Meng, D., Forai, P., Huang, Y.S., Long, Q., Segura, V.,**
1054 **and Nordborg, M.** (2012). GWAPP: a web application for genome-wide association mapping in
1055 *Arabidopsis*. *Plant Cell* **24**, 4793-4805.

1056 **Shen, X., Pettersson, M., Ronnegard, L., and Carlborg, O.** (2012). Inheritance beyond plain heritability:
1057 variance-controlling genes in *Arabidopsis thaliana*. *PLoS Genet.* **8**, e1002839.

1058 **Si, L., et al.** (2016). OsSPL13 controls grain size in cultivated rice. *Nat. Genet.* **48**, 447-456.

1059 **Sun, H., et al.** (2014). Heterotrimeric G proteins regulate nitrogen-use efficiency in rice. *Nat. Genet.*

1060 **Swamy, B.P.M., Rahman, M.A., Inabangan-Asilo, M.A., Amparado, A., Manito, C.,**
1061 **Chadha-Mohanty, P., Reinke, R., and Slamet-Loedin, I.H.** (2016). Advances in breeding for high
1062 grain Zinc in Rice. *Rice (N Y)* **9**, 49.

1063 **Tomatsu, H., Takano, J., Takahashi, H., Watanabe-Takahashi, A., Shibagaki, N., and Fujiwara, T.**
1064 (2007). An *Arabidopsis thaliana* high-affinity molybdate transporter required for efficient uptake of
1065 molybdate from soil. *Proc. Natl. Acad. Sci. U. S. A.* **104**, 18807-18812.

1066 **Tomcal, M., Stiffler, N., and Barkan, A.** (2013). POGs2: a web portal to facilitate cross-species
1067 inferences about protein architecture and function in plants. *PLoS One* **8**, e82569.

1068 **Trijatmiko, K.R., et al.** (2016). Biofortified *indica* rice attains iron and zinc nutrition dietary targets in the
1069 field. *Sci. Rep.* **6**, 19792.

1070 **Ueno, D., Yamaji, N., Kono, I., Huang, C.F., Ando, T., Yano, M., and Ma, J.F.** (2010). Gene limiting
1071 cadmium accumulation in rice. *Proc. Natl. Acad. Sci. U. S. A.* **107**, 16500-16505.

1072 **Ueno, D., Milner, M.J., Yamaji, N., Yokosho, K., Koyama, E., Clemencia Zambrano, M., Kaskie, M.,**
1073 **Ebbs, S., Kochian, L.V., and Ma, J.F.** (2011). Elevated expression of TcHMA3 plays a key role in the
1074 extreme Cd tolerance in a Cd-hyperaccumulating ecotype of *Thlaspi caerulescens*. *Plant J.* **66**,
1075 852-862.

1076 **Uraguchi, S., and Fujiwara, T.** (2013). Rice breaks ground for cadmium-free cereals. *Curr. Opin. Plant*
1077 *Biol.* **16**, 328-334.

1078 **Van Bel, M., Proost, S., Wischnitzki, E., Movahedi, S., Scheerlinck, C., Van de Peer, Y., and**
1079 **Vandepoele, K.** (2012). Dissecting plant genomes with the PLAZA comparative genomics platform.
1080 *Plant Physiol.* **158**, 590-600.

1081 **Wang, Q., Xie, W., Xing, H., Yan, J., Meng, X., Li, X., Fu, X., Xu, J., Lian, X., Yu, S., Xing, Y., and**
1082 **Wang, G.** (2015). Genetic architecture of natural variation in rice chlorophyll content revealed by
1083 genome wide association study. *Mol Plant.*

1084 **Wei, D., Cui, K.H., Ye, G.Y., Pan, J.F., Xiang, J., Huang, J.L., and Nie, L.X.** (2012). QTL mapping for
1085 nitrogen-use efficiency and nitrogen-deficiency tolerance traits in rice. *Plant Soil* **359**, 281-295.

1086 **Wei, X.J., Xu, J.F., Guo, H.N., Jiang, L., Chen, S.H., Yu, C.Y., Zhou, Z.L., Hu, P.S., Zhai, H.Q., and**
1087 **Wan, J.M.** (2010). DTH8 Suppresses Flowering in Rice, Influencing Plant Height and Yield Potential
1088 Simultaneously. *Plant Physiol.* **153**, 1747-1758.

1089 **Weng, X.Y., Wang, L., Wang, J., Hu, Y., Du, H., Xu, C.G., Xing, Y.Z., Li, X.H., Xiao, J.H., and Zhang,**
1090 **Q.F.** (2014). Grain Number, Plant Height, and Heading Date7 Is a Central Regulator of Growth,

1091 Development, and Stress Response. *Plant Physiol.* **164**, 735-747.

1092 **White, P.J., and Broadley, M.R.** (2009). Biofortification of crops with seven mineral elements often
 1093 lacking in human diets - iron, zinc, copper, calcium, magnesium, selenium and iodine. *New Phytol.*
 1094 **182**, 49-84.

1095 **Williams, L., and Salt, D.E.** (2009). The plant ionome coming into focus. *Curr. Opin. Plant Biol.* **12**,
 1096 247-249.

1097 **Withers, P.J.A., and Lord, E.I.** (2002). Agricultural nutrient inputs to rivers and groundwaters in the UK:
 1098 policy, environmental management and research needs. *Sci. Total Environ.* **282**, 9-24.

1099 **Xie, W., et al.** (2015). Breeding signatures of rice improvement revealed by a genomic variation map from
 1100 a large germplasm collection. *Proc. Natl. Acad. Sci. U. S. A.* **112**, E5411-5419.

1101 **Xue, W.Y., Xing, Y.Z., Weng, X.Y., Zhao, Y., Tang, W.J., Wang, L., Zhou, H.J., Yu, S.B., Xu, C.G., Li,**
 1102 **X.H., and Zhang, Q.F.** (2008). Natural variation in *Ghd7* is an important regulator of heading date
 1103 and yield potential in rice. *Nat. Genet.* **40**, 761-767.

1104 **Yan, W.H., Wang, P., Chen, H.X., Zhou, H.J., Li, Q.P., Wang, C.R., Ding, Z.H., Zhang, Y.S., Yu, S.B.,**
 1105 **Xing, Y.Z., and Zhang, Q.F.** (2011). A major QTL, *Ghd8*, plays pleiotropic roles in regulating grain
 1106 productivity, plant height, and heading date in rice. *Molecular plant* **4**, 319-330.

1107 **Yang, M., Zhang, Y., Zhang, L., Hu, J., Zhang, X., Lu, K., Dong, H., Wang, D., Zhao, F.J., Huang,**
 1108 **C.F., and Lian, X.** (2014). *OsNRAMP5* contributes to manganese translocation and distribution in rice
 1109 shoots. *J. Exp. Bot.* **65**, 4849-4861.

1110 **Yano, K., Yamamoto, E., Aya, K., Takeuchi, H., Lo, P.C., Hu, L., Yamasaki, M., Yoshida, S., Kitano,**
 1111 **H., Hirano, K., and Matsuoka, M.** (2016). Genome-wide association study using whole-genome
 1112 sequencing rapidly identifies new genes influencing agronomic traits in rice. *Nat. Genet.* **48**, 927-934.

1113 **Yoshida, S., Forno, D.A., Cock, J.H., and Gomez, K.A.** (1976). *Laboratory Manual for Physiological*
 1114 *Studies of Rice*, 3rd ed. International Rice Research Institute, Manila.

1115 **Yu, S.B., Xu, W.J., Vijayakumar, C.H., Ali, J., Fu, B.Y., Xu, J.L., Jiang, Y.Z., Marghirang, R.,**
 1116 **Domingo, J., Aquino, C., Virmani, S.S., and Li, Z.K.** (2003). Molecular diversity and multilocus
 1117 organization of the parental lines used in the International Rice Molecular Breeding Program. *Theor.*
 1118 *Appl. Genet.* **108**, 131-140.

1119 **Zhang, H., Zhang, D., Wang, M., Sun, J., Qi, Y., Li, J., Wei, X., Han, L., Qiu, Z., Tang, S., and Li, Z.**
 1120 (2011). A core collection and mini core collection of *Oryza sativa* L. in China. *Theor. Appl. Genet.* **122**,
 1121 49-61.

1122 **Zhang, M., Pinson, S.R., Tarpley, L., Huang, X.Y., Lahner, B., Yakubova, E., Baxter, I., Guerinot,**
 1123 **M.L., and Salt, D.E.** (2014). Mapping and validation of quantitative trait loci associated with
 1124 concentrations of 16 elements in unmilled rice grain. *Theor. Appl. Genet.* **127**, 137-165.

1125 **Zhang, J., et al.** (2015). Combinations of the *Ghd7*, *Ghd8* and *Hd1* genes largely define the
 1126 ecogeographical adaptation and yield potential of cultivated rice. *New Phytol.* **208**, 1056-1066.

1127 **Zhao, F.J., McGrath, S.P., and Meharg, A.A.** (2010). Arsenic as a Food Chain Contaminant:
 1128 Mechanisms of Plant Uptake and Metabolism and Mitigation Strategies. *Annu. Rev. Plant Biol.* **61**,
 1129 535-559.

1130 **Zhao, H., Yao, W., Ouyang, Y., Yang, W., Wang, G., Lian, X., Xing, Y., Chen, L., and Xie, W.** (2014).
 1131 RiceVarMap: a comprehensive database of rice genomic variations. *Nucleic Acids Res.*

1132

1133

1134 **FIGURE LEGENDS**

1135 **Figure 1.** Hierarchical clustering on field conditions, subpopulations and tissues based
1136 on the ionome of a natural population of cultivated rice.

1137 The clustering was performed using centralized concentrations of each element.

1138

1139 **Figure 2.** Presentation of a few well reproducible and significant Manhattan and Q-Q
1140 plots for these elements.

1141 The first part of the title for each panel indicates the elemental types; the second part
1142 represents the location from which it was scanned; the third part shows its tissue types
1143 [specially at Wuhan: the first letter indicate field types ("C", "N" and "P" means "NF",
1144 "LN field" and "LP field" respectively); the second and third letter represent tissue types
1145 (HS: shoots at heading stage; MS: shoots at maturation stage; MG: brown rice)]; the last
1146 part represents subpopulation types (Ind: *indica*; Jap: *japonica*). Red arrows pointed to
1147 the loci repeatedly scanned in different field trials.

1148

1149 **Figure 3.** Distribution of 72 common loci which were repeatedly scanned within or
1150 across locations on 12 chromosomes according to physical distance.

1151 The number on the left side of the column represents the physical location (Mb) of each
1152 lead SNP. The letters to the right of the column represent the corresponding elements.
1153 Different color referred to different location from which the locus was scanned. Blue,
1154 Wuhan; green, Youxian; red, both locations. Underline indicated the locus scanned at
1155 Wuhan by all three fields or at Youxian by all two fields. One and two asterisks implied
1156 the locus was not only scanned across location but also repeatedly scanned within one
1157 and two locations respectively. The Venn diagram displayed the numbers of repeated loci
1158 within or across locations.

1159

1160 **Figure 4.** GWAS for Na concentration and identification of the candidate gene
1161 *Os-HKT1;5* for the repeatedly scanned locus on chromosome 1.

1162 (A) and (B) Manhattan and Q-Q plots for straw Na concentrations in *indica*
1163 subpopulation at locations of Wuhan (A; LP field) and Youxian (B; 2015), respectively.
1164 Red arrows pointed to the lead SNPs which were located close to *Os-HKT1;5*.

1165 (C) Gene model of *Os-HKT1;5*. Filled black boxes represented coding sequence. The
1166 gray vertical lines marked the polymorphic sites identified by high-throughput
1167 sequencing, and the star represented the potentially functional site.

1168 (D) A representation of pairwise r^2 values (a measure of LD) among all polymorphic sites
1169 in *Os-HKT1;5*, where the darkness of the color of each box corresponded to the r^2 value
1170 according to the legend.

1171 (E) A list for 9 SNPs which led to 9 amino-acid changes in coding sequence of
1172 *Os-HKT1;5*. Red contents indicated the four variations previously identified. The two
1173 asterisks indicated the SNP showing strong linkage with lead SNP of this locus.

1174 (F) to (J) Box plot for Na concentrations in straws at SNP sf0111461701. F, normal field
1175 at Wuhan; G, LN field at Wuhan; H, LP field at Wuhan; I, 2014 at Youxian; J, 2015 at
1176 Youxian.

1177

1178 **Figure 5.** Analysis of Na concentrations in different *Os-HKT1;5* haplotypes in our
1179 collection.

1180 Significant differences at $P < 0.05$ within each group are indicated by different letters
1181 (one way ANOVA test).

1182

1183 **Figure 6.** Characterization of *Os-MOT1;1* by GWAS.

1184 (A) and (B) Manhattan and Q-Q plots displaying the GWAS result of Mo concentrations
1185 of straw in *indica* subpopulation at Wuhan (LP field; A) and Youxian (2014; B)

1186 respectively.

1187 **(C)** Gene model of *Os-MOT1;1*. Filled black boxes represented the coding sequence. The
1188 gray vertical lines marked the polymorphic sites identified by high-throughput
1189 sequencing, and the stars represented the potentially functional site.

1190 **(D)** A representation of pairwise r^2 values (a measure of LD) among all polymorphic sites
1191 in *Os-MOT1;1*, where the darkness of the color of each box corresponded to the r^2 value
1192 according to the legend.

1193 **(E) to (I)** Box plot for Mo concentrations of *indica* subpopulation in different field
1194 conditions at SNP sf0800008059.

1195 **(J)** Detecting the difference of *Os-MOT1;1* promoter region by PCR. Blue and red
1196 horizontal line indicated fragments from T type and C type of *indica* accessions at SNP
1197 sf0800008059, respectively.

1198 **(K)** Schematic presentation of the genomic structure and sequence variations of
1199 *Os-MOT1;1* in T type and C type of *indica* accessions at SNP sf0800008059. The
1200 *Os-MOT1;1* sequence of Nipponbare downloaded from rice annotation database of
1201 Michigan State University (MSU) was used as the reference sequence. The *Os-MOT1;1*
1202 sequences of T type and C type of *indica* accessions at SNP sf0800008059 were based on
1203 a fully sequenced data of 10 accessions in each type. The black filled boxes in the
1204 promoter and CDS regions, open triangles and short vertical lines indicated sequence
1205 deletions, insertions and single base mutations, respectively.

1206 **(L) and (M)** *Os-MOT1;1* expression at roots of different types of *indica* accessions under
1207 Mo sufficient condition **(L)** and Mo deficient condition **(M)**. Data are shown as the
1208 means of three biological replicates \pm SD, and roots of three plants were mixed in one
1209 replication. The *P* value is calculated using the *t* approximation.

1210

1211 **Figure 7.** Functional analysis of *Os-MOT1;1* based on transgenic plants.

1212 **(A)** Schematic presentation of four kinds of *Os-MOT1;1* CDS used for constructing

1213 over-expressed rice plants. The vertical thick lines represented sequence deletions or
1214 single base mutations.

1215 **(B)** The expression levels of *Os-MOT1;1* in wild-type (Zhonghua 11) and transgenic
1216 lines by qRT-PCR. Six transgenic lines of each type *Os-MOT1;1* were analyzed, and
1217 among these, three lines possessed relative low expression levels and the other three
1218 possessed relative high expression levels. Data are shown as the means of three
1219 biological replicates \pm SD, and leaf blade from three plants were mixed in one
1220 replication.

1221 **(C)** and **(D)** The determination of Mo concentrations in roots **(C)** and shoots **(D)** of
1222 wild-type and transgenic plants. Data are shown as the means of three biological
1223 replicates \pm SD, and roots or shoots of three plants were mixed in one replication.
1224 Significant differences at $P < 0.05$ among different groups are indicated by different
1225 letters (one way ANOVA test).

1226 **(E)** and **(F)** Scatter plot for Mo concentrations and expression levels of *Os-MOT1;1* in
1227 roots **(E)** and shoots **(F)** of wild-type and transgenic plants.

1228

1229 **Figure 8.** Characterization of *Ghd7* in rice N accumulation by GWAS.

1230 **(A)** Manhattan and Q-Q plots displaying the GWAS results of N concentrations in shoots
1231 of *indica* subpopulation at heading stage at LP field in Wuhan.

1232 **(B)** Manhattan and Q-Q plots displaying the GWAS results of heading dates of *indica*
1233 subpopulation.

1234 **(C)** Manhattan and Q-Q plots displaying the GWAS results of N concentrations in shoots
1235 of *indica* subpopulation at heading stage at LP field in Wuhan by using heading dates as
1236 a covariate. Red arrows in **A**, **B** and **C** pointed to a same lead SNP which was located
1237 close to *Ghd7*.

1238 **(D)** Gene model of *Ghd7*. The black filled boxes represented coding sequence. The gray
1239 vertical lines marked the polymorphic sites identified by high-throughput sequencing in

1240 *indica* subspecies.

1241 **(E)** Haplotype analysis of *Ghd7* gene region in *indica* subspecies based on polymorphic
1242 sites shown in **D**. Only haplotypes with total number of accessions ≥ 5 were analyzed.

1243 **(F)** Box plot for heading dates of different *Ghd7* haplotypes.

1244 **(G)** to **(I)** Box plots for shoot N concentrations of different *Ghd7* haplotypes at heading
1245 stage in normal field (**G**), LN field (**H**) and LP field (**I**) in Wuhan. Significant differences
1246 at $P < 0.05$ within each group are indicated by different letters (one way ANOVA test).

1247

1248 **Figure 9.** Functional identification of *Ghd7* in rice N accumulation based on
1249 near-isogenic lines and transgenic plants.

1250 **(A)** to **(C)** N concentrations in shoots at heading stage (**A**), in straw (**B**) and in brown rice
1251 (**C**), of four near-isogenic lines.

1252 **(D)** to **(F)** N concentrations in shoots at heading stage (**D**), in straw (**E**) and in brown rice
1253 (**F**), of wild type and transgenic plants.

1254 Data are shown as the means of three biological replicates \pm SD, and corresponding
1255 tissues of five plants were mixed in one replication for metal determination. Two
1256 asterisks indicate significant differences ($P < 0.01$) compared with the wild type (*t* test).

1257

1258

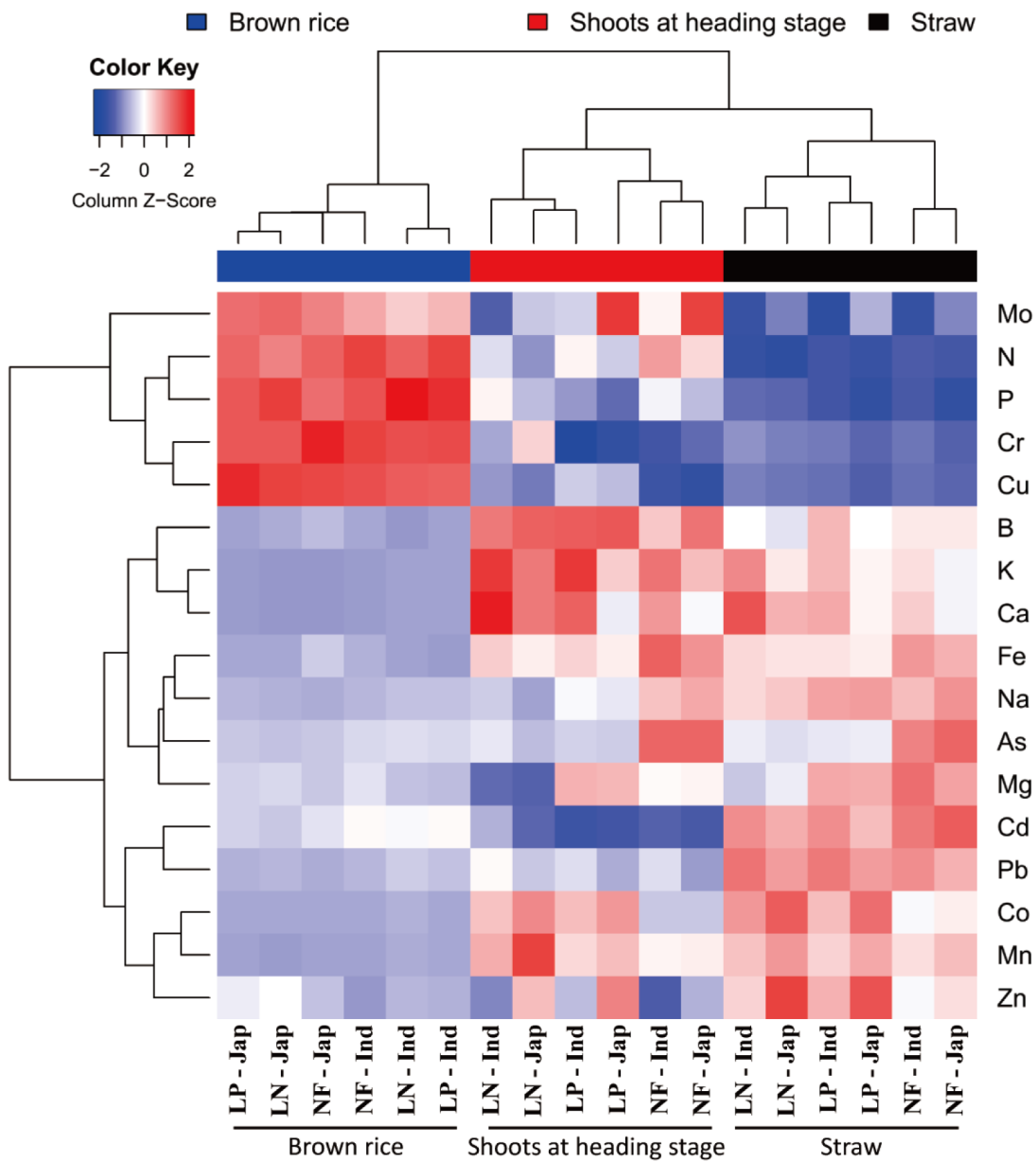


Figure 1. Hierarchical clustering on field conditions, subpopulations and tissues based on the ionome of a natural population of cultivated rice. The clustering was performed using centralized concentrations of each element.

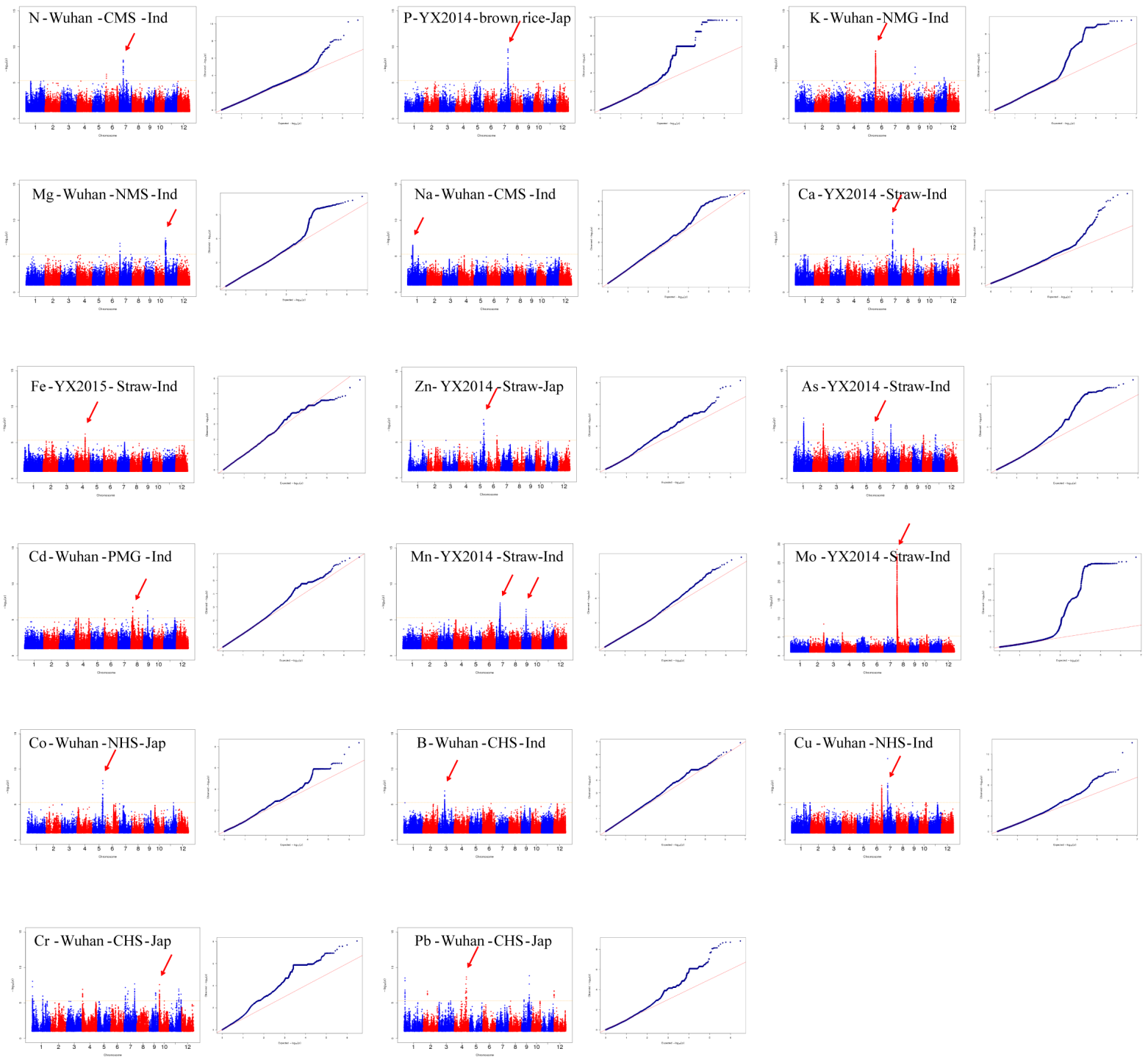


Figure 2. Presentation of a few well reproducible and significant Manhattan and Q-Q plots for these elements. The first part of the title for each panel indicates the elemental types; the second part represents the location from which it was scanned; the third part shows its tissue types [specially in Wuhan: the first letter indicate field types ("C", "N" and "P" means "NF", "LN field" and "LP field" respectively); the second and third letter represent tissue types (HS: shoots at heading stage; MS: shoots at maturation stage; MG: brown rice)]; the last part represents subpopulation types (Ind: *indica*; Jap: *japonica*). Red arrows pointed to the loci repeatedly scanned in different field trials.

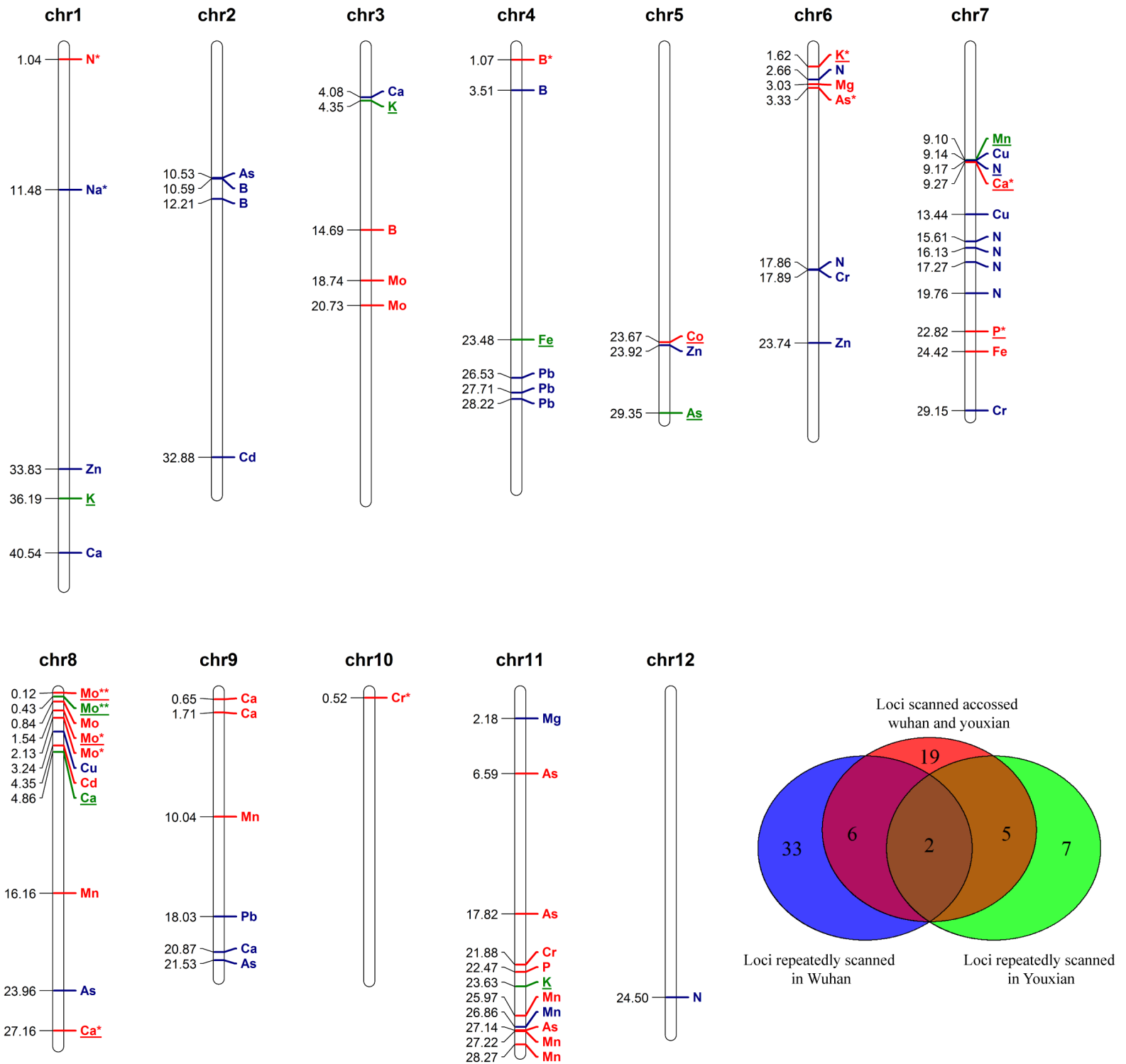


Figure 3. Figure 3. Distribution of 72 common loci which were repeatedly scanned within or across locations on 12 chromosomes according to physical distance.

The number on the left side of the column represents the physical location (Mb) of each lead SNP. The letters to the right of the column represent the corresponding elements. Different color referred to different location from which the locus was scanned. Blue, Wuhan; green, Youxian; red, both locations. Underline indicated the locus scanned in Wuhan by all three fields or in Youxian by all two fields. One and two asterisks implied the locus was not only scanned across location but also repeatedly scanned within one and two locations respectively. The Venn diagram displayed the numbers of repeated loci within or across locations.

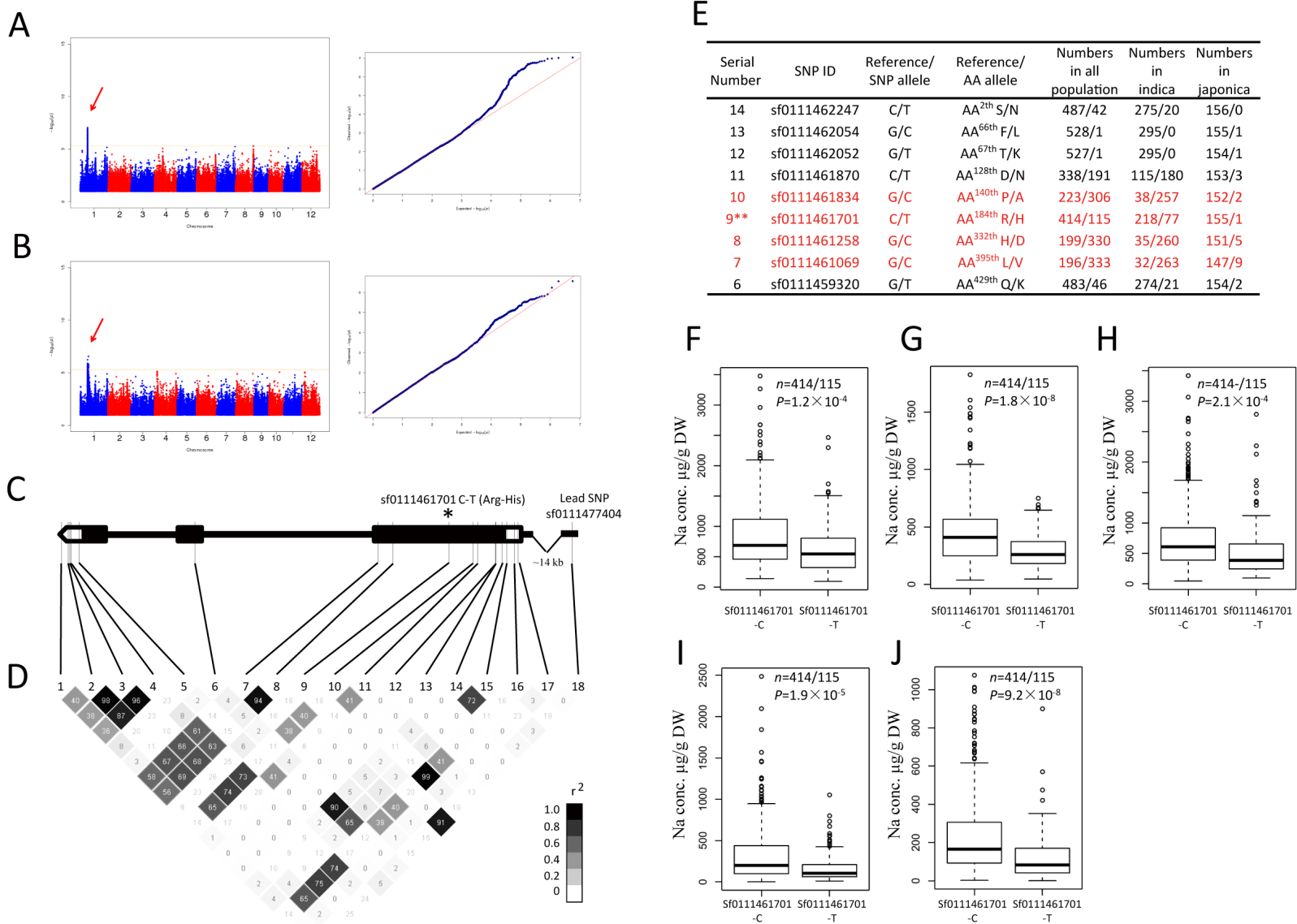


Figure 4. GWAS for Na concentration and identification of the candidate gene *Os-HKT1;5* for the repeatedly scanned locus on chromosome 1.

(A) and (B) Manhattan and Q-Q plots for straw Na concentrations in *indica* subpopulation at locations of Wuhan (A; LP field) and Youxian (B; 2015), respectively. Red arrows pointed to the lead SNPs which were located close to *Os-HKT1;5*.

(C) Gene model of *Os-HKT1;5*. Filled black boxes represented coding sequence. The gray vertical lines marked the polymorphic sites identified by high-throughput sequencing, and the star represented the potentially functional site.

(D) A representation of pairwise r^2 values (a measure of LD) among all polymorphic sites in *Os-HKT1;5*, where the darkness of the color of each box corresponded to the r^2 value according to the legend.

(E) A list for 9 SNPs which led to 9 amino-acid changes in coding sequence of *Os-HKT1;5*. Red contents indicated the four variations previously identified. The two asterisks indicated the SNP showing strong linkage with lead SNP of this locus.

(F) to (J) Box plot for Na concentrations in straws at SNP sf0111461701. F, normal field at Wuhan; G, LN field at Wuhan; H, LP field at Wuhan; I, Youxian at 2014; J, Youxian at 2015.

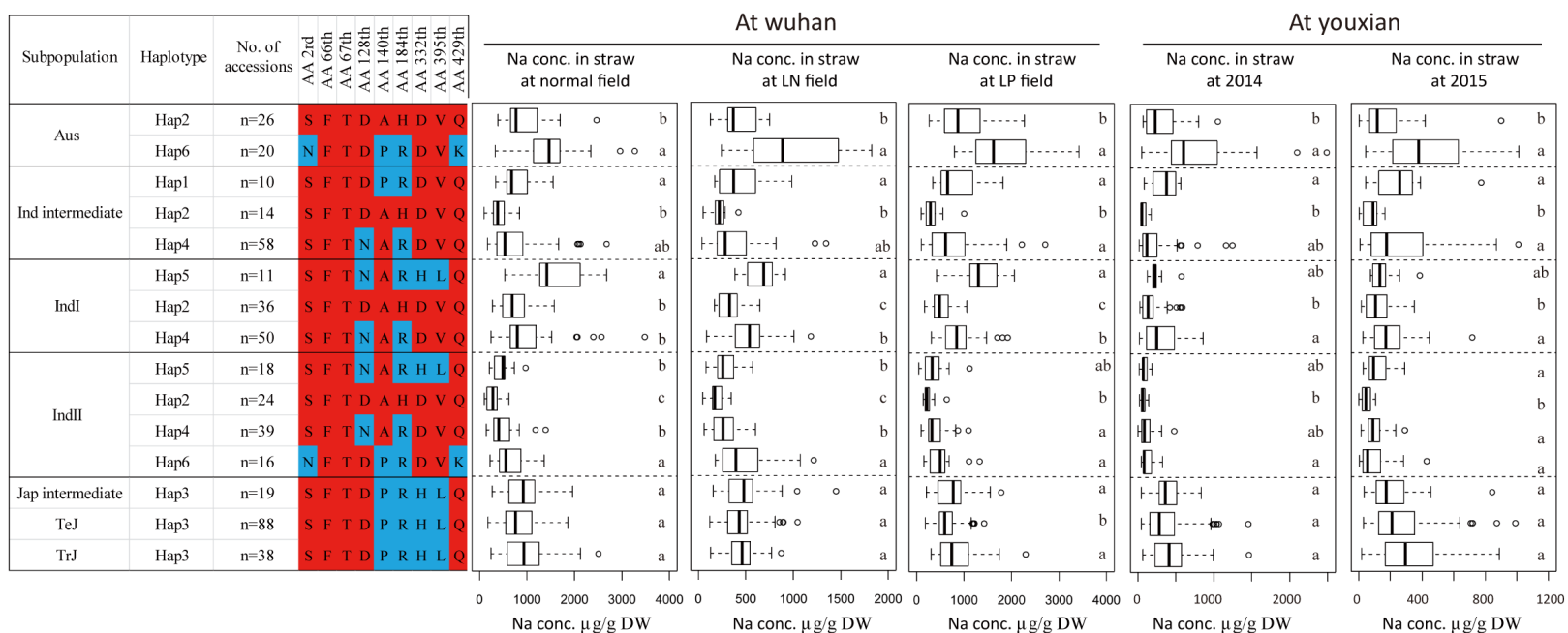


Figure 5. Analysis of Na concentrations in different Os-HKT1;5 haplotypes in our collection. Significant differences at $P < 0.05$ within each group are indicated by different letters (one way ANOVA test).

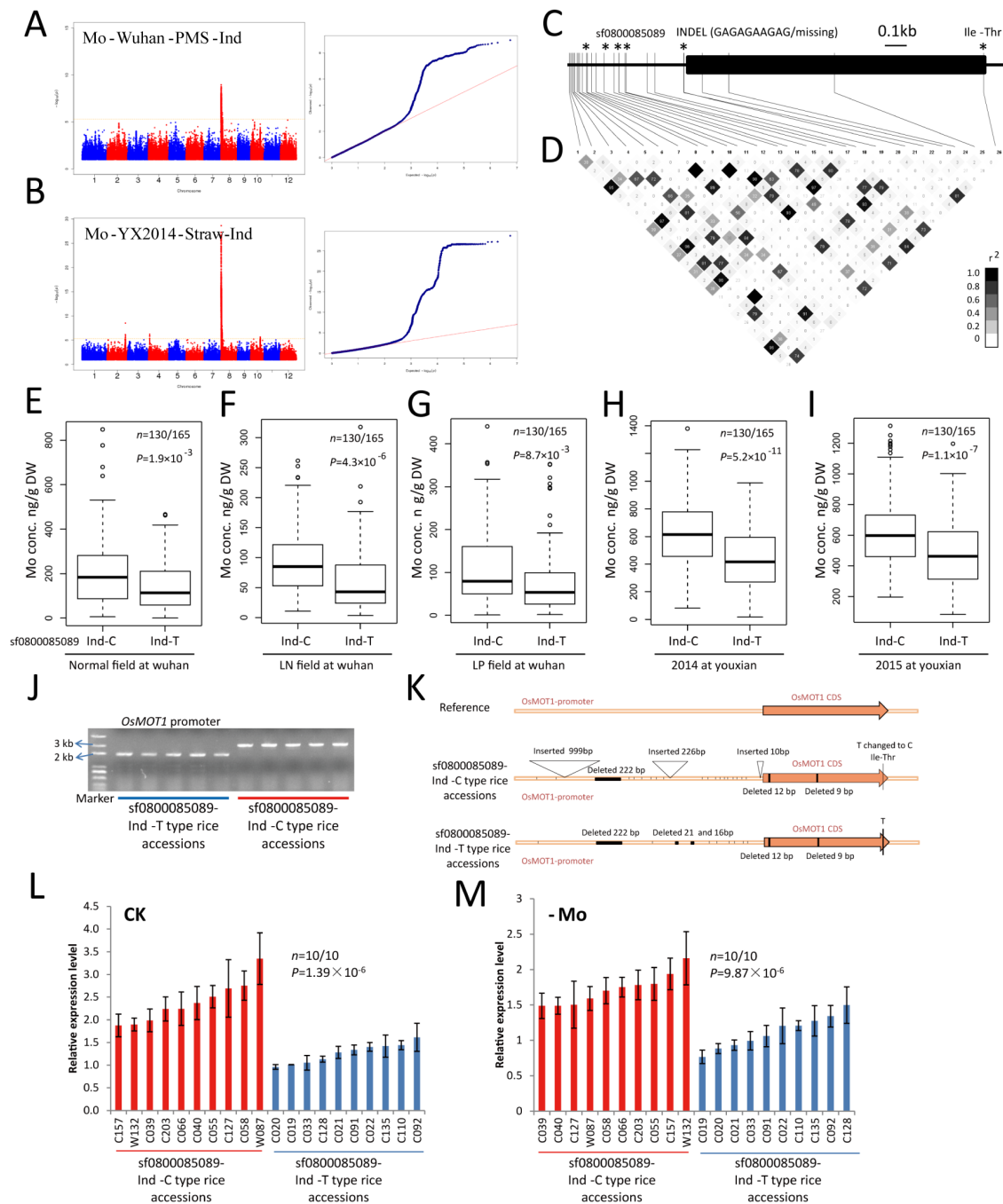


Figure 6. Characterization of *Os-MOT1;1* by GWAS.

(A) and (B) Manhattan and Q-Q plots displaying the GWAS result of Mo concentrations of straw in *indica* subpopulation at Wuhan (LP field; A) and Youxian (2014; B) respectively.

(C) Gene model of *Os-MOT1;1*. Filled black boxes represented the coding sequence. The gray vertical lines marked the polymorphic sites identified by high-throughput sequencing, and the stars represented the potentially functional site.

(D) A representation of pairwise r^2 values (a measure of LD) among all polymorphic sites in *Os-MOT1;1*, where the darkness of the color of each box corresponded to the r^2 value according to the legend.

(E) to (I) Box plot for Mo concentrations of indica subpopulation in different field conditions at SNP sf0800008059.

(J) Detecting the difference of *Os-MOT1;1* promoter region by PCR. Blue and red horizontal line indicated fragments from T type and C type of *indica* accessions at SNP sf0800008059, respectively.

(K) Schematic presentation of the genomic structure and sequence variations of *Os-MOT1;1* in T type and C type of *indica* accessions at SNP sf0800008059. The *Os-MOT1;1* sequence of Nipponbare downloaded from rice annotation database of Michigan State University (MSU) was used as the reference sequence. The *Os-MOT1;1* sequences of T type and C type of *indica* accessions at SNP sf0800008059 were based on a fully sequenced data of 10 accessions in each type. The black filled boxes in the promoter and CDS regions, open triangles and short vertical lines indicated sequence deletions, insertions and single base mutations, respectively.

(L) and (M) *Os-MOT1;1* expression at roots of different types of *indica* accessions under Mo sufficient condition (L) and Mo deficient condition (M). Data are shown as the means of three biological replicates \pm SD, and roots of three plants were mixed in one replication. The P value is calculated using the t approximation.

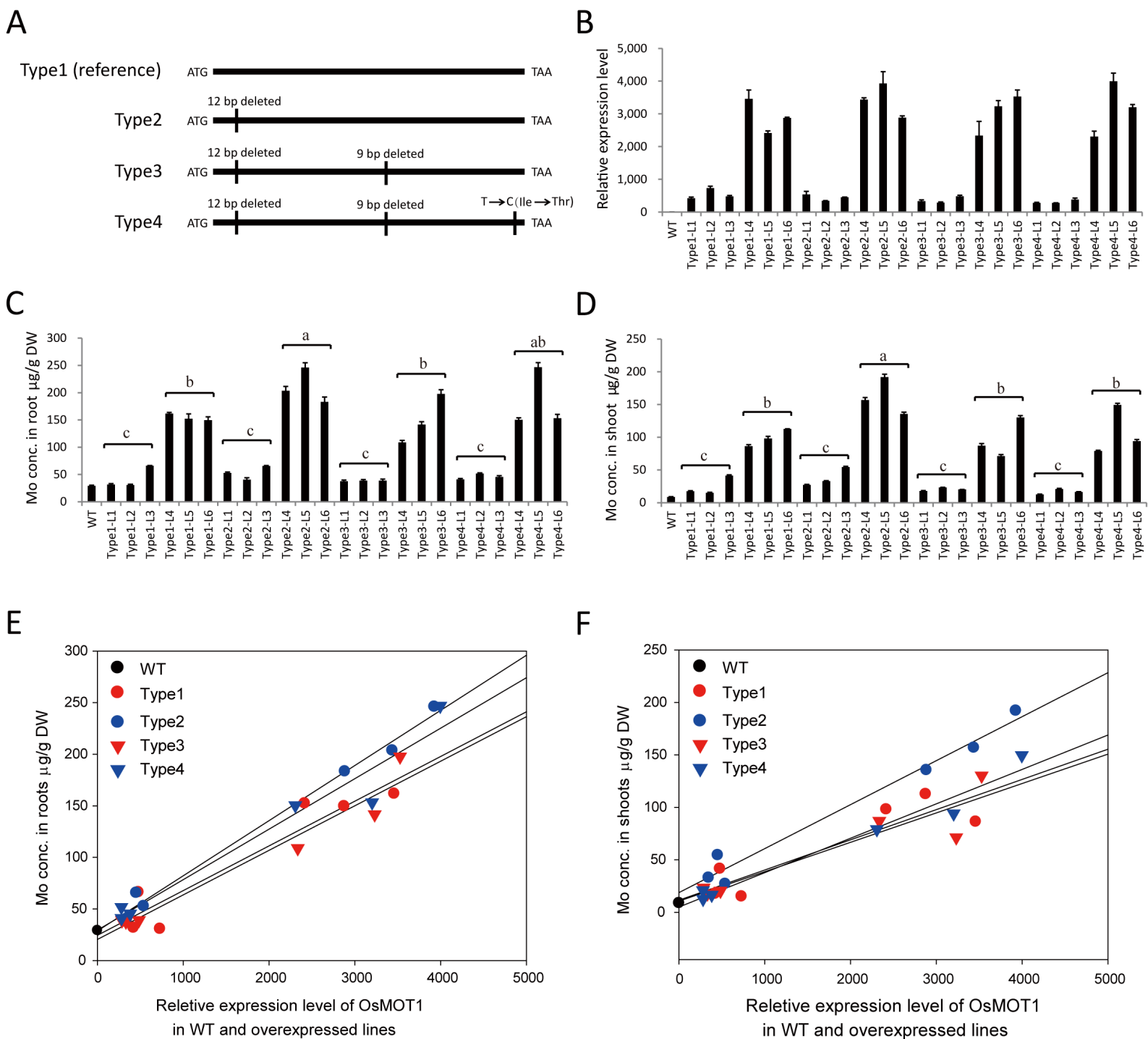


Figure 7. Functional analysis of *Os-MOT1;1* based on transgenic plants.

(A) Schematic presentation of four kinds of *Os-MOT1;1* CDS used for constructing over-expressed rice plants. The vertical thick lines represented sequence deletions or single base mutations.

(B) The expression levels of *Os-MOT1;1* in wild-type (Zhonghua 11) and transgenic lines by qRT-PCR. Six transgenic lines of each type *Os-MOT1;1* were analyzed, and among these, three lines possessed relative low expression levels and the other three possessed relative high expression levels. Data are shown as the means of three biological replicates \pm SD, and leaf blade from three plants were mixed in one replication.

(C) and (D) The determination of Mo concentrations in roots (C) and shoots (D) of wild-type and transgenic plants. Data are shown as the means of three biological replicates \pm SD, and roots or shoots of three plants were mixed in one replication. Significant differences at $P < 0.05$ among different groups are indicated by different letters (one way ANOVA test).

(E) and (F) Scatter plot for Mo concentrations and expression levels of *Os-MOT1;1* in roots (E) and shoots (F) of wild-type and transgenic plants.

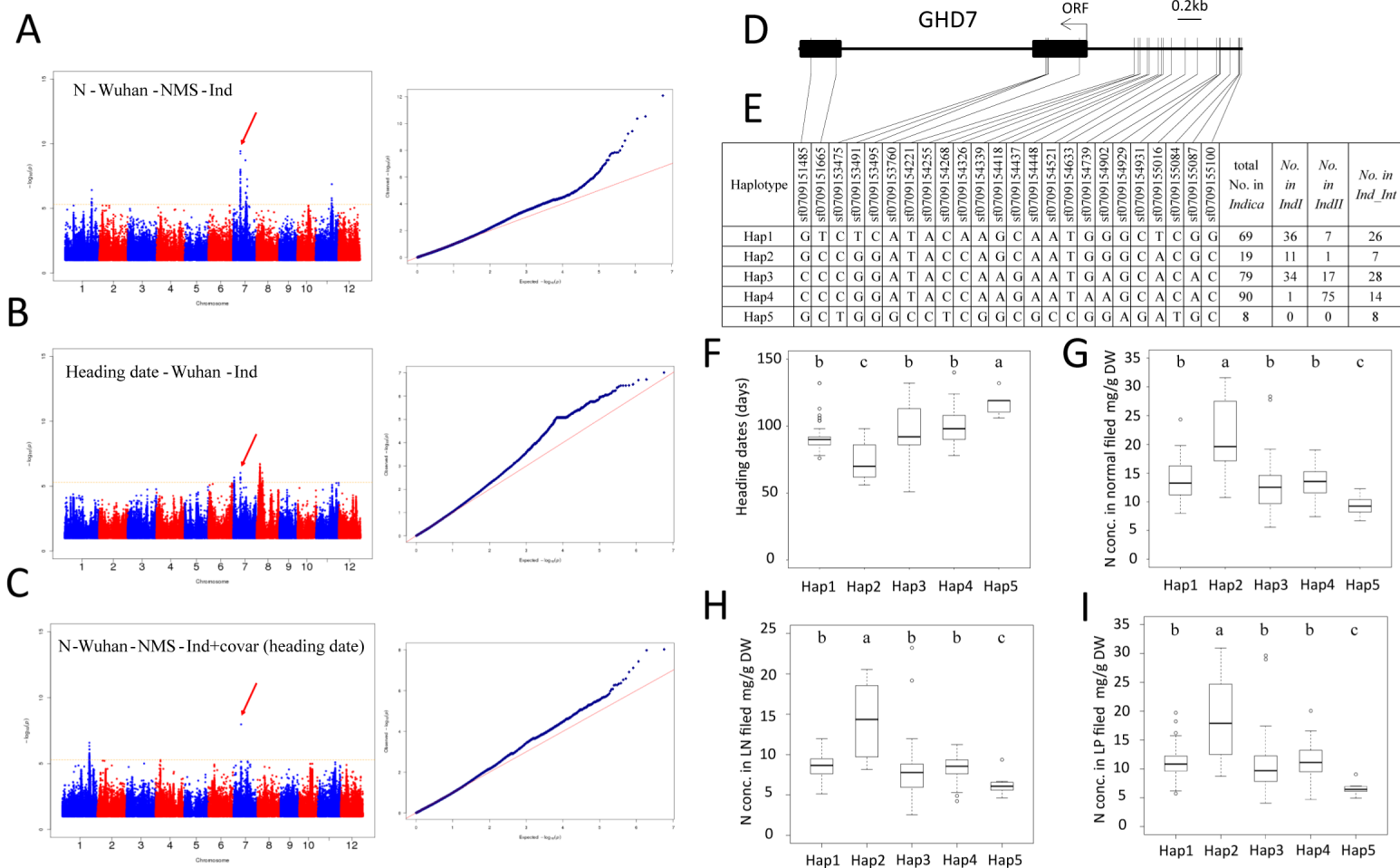


Figure 8. Characterization of *Ghd7* in rice N accumulation by GWAS.

(A) Manhattan and Q-Q plots displaying the GWAS results of N concentrations in shoots of *indica* subpopulation at heading stage at LP field in Wuhan.

(B) Manhattan and Q-Q plots displaying the GWAS results of heading dates of *indica* subpopulation.

(C) Manhattan and Q-Q plots displaying the GWAS results of N concentrations in shoots of *indica* subpopulation at heading stage at LP field in Wuhan by using heading dates as a covariate. Red arrows in A, B and C pointed to the lead SNPs which were located close to *Ghd7*.

(D) Gene model of *Ghd7*. The black filled boxes represented coding sequence. The gray vertical lines marked the polymorphic sites identified by high-throughput sequencing in *indica* subspecies.

(E) Haplotype analysis of *Ghd7* gene region in *indica* subspecies based on polymorphic sites shown in D. Only haplotypes with total number of accessions ≥ 5 were analyzed.

(F) Box plot for heading dates of different *Ghd7* haplotypes.

(G) to (I) Box plots for shoot N concentrations of different *Ghd7* haplotypes at heading stage in normal field (G), LN field (H) and LP field (I) in Wuhan. Significant differences at $P < 0.05$ within each group are indicated by different letters (one way ANOVA test).

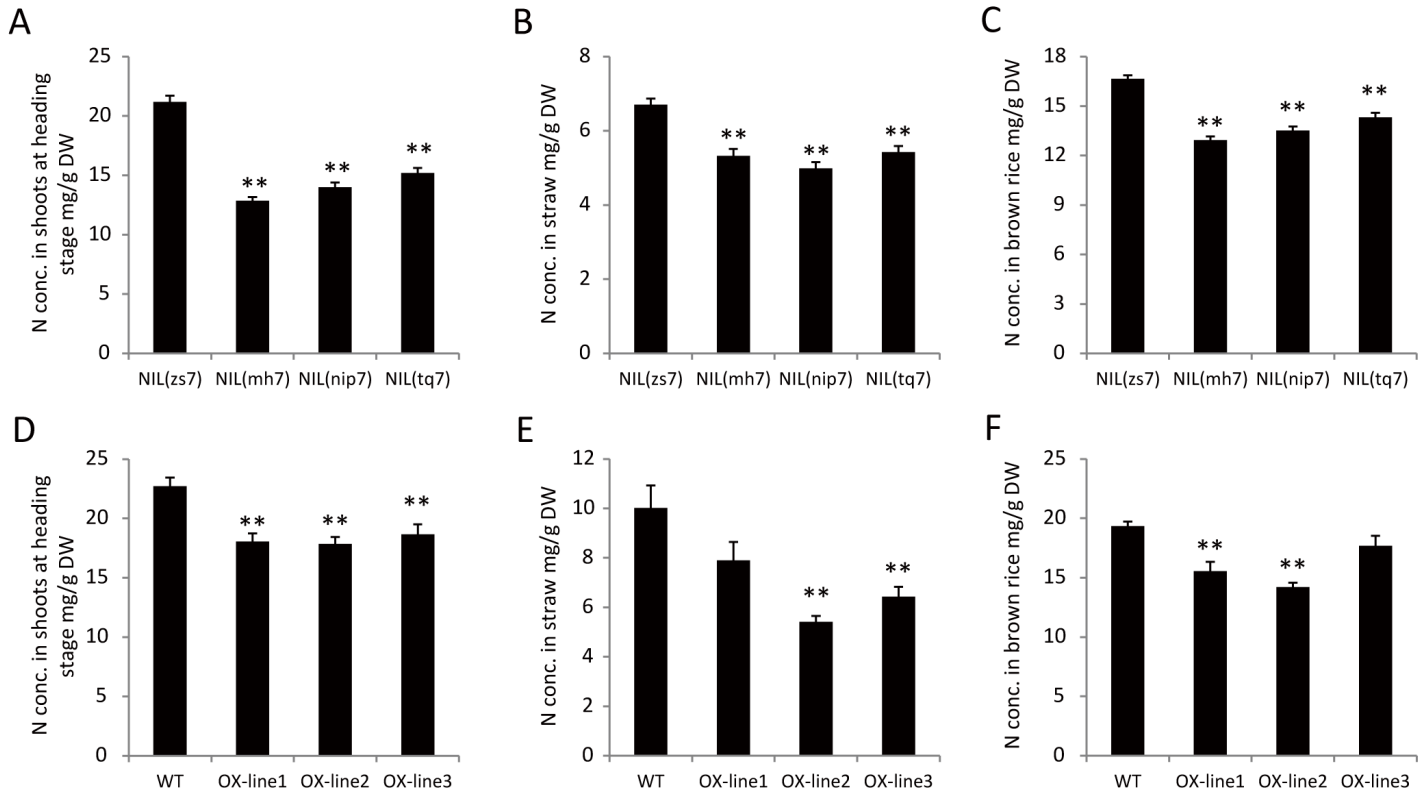


Figure 9. Functional identification of *Ghd7* in rice N accumulation based on near-isogenic lines and transgenic plants.

(A) to (C) N concentrations in shoots at heading stage (A), in straw (B) and in brown rice (C), of four near-isogenic lines.

(D) to (F) N concentrations in shoots at heading stage (D), in straw (E) and in brown rice (F), of wild type and transgenic plants.

Data are shown as the means of three biological replicates \pm SD, and corresponding tissues of five plants were mixed in one replication for metal determination. Two asterisks indicate significant differences ($P < 0.01$) compared with the wild type (t test).

Parsed Citations

Agrama, H.A., Yan, W.G., Lee, F., Fjellstrom, R., Chen, M.H., Jia, M., and McClung, A. (2009). Genetic Assessment of a Mini-Core Subset Developed from the USDA Rice Genebank. *Crop Sci.* 49, 1336-1346.

Pubmed: [Author and Title](#)

CrossRef: [Author and Title](#)

Google Scholar: [Author Only](#) [Title Only](#) [Author and Title](#)

Arao, T., and Ae, N. (2003). Genotypic variations in cadmium levels of rice grain. *Soil Sci. Plant Nutr.* 49, 473-479.

Pubmed: [Author and Title](#)

CrossRef: [Author and Title](#)

Google Scholar: [Author Only](#) [Title Only](#) [Author and Title](#)

Asaro, A., Ziegler, G., Ziyomo, C., Hoekenga, O.A., Dilkes, B.P., and Baxter, I. (2016). The Interaction of Genotype and Environment Determines Variation in the Maize Kernel Ionome. *G3 (Bethesda, Md.)* 6, 4175-4183.

Pubmed: [Author and Title](#)

CrossRef: [Author and Title](#)

Google Scholar: [Author Only](#) [Title Only](#) [Author and Title](#)

Axelsen, K.B., and Palmgren, M.G. (2001). Inventory of the superfamily of P-type ion pumps in Arabidopsis. *Plant Physiol.* 126, 696-706.

Pubmed: [Author and Title](#)

CrossRef: [Author and Title](#)

Google Scholar: [Author Only](#) [Title Only](#) [Author and Title](#)

Barrett, J.C. (2009). Haploview: Visualization and analysis of SNP genotype data. *Cold Spring Harb Protoc* 2009, pdb ip71.

Pubmed: [Author and Title](#)

CrossRef: [Author and Title](#)

Google Scholar: [Author Only](#) [Title Only](#) [Author and Title](#)

Baxter, I., Hermans, C., Lahner, B., Yakubova, E., Tikhonova, M., Verbruggen, N., Chao, D.Y., and Salt, D.E. (2012). Biodiversity of mineral nutrient and trace element accumulation in Arabidopsis thaliana. *PLoS One* 7, e35121.

Pubmed: [Author and Title](#)

CrossRef: [Author and Title](#)

Google Scholar: [Author Only](#) [Title Only](#) [Author and Title](#)

Baxter, I., Muthukumar, B., Park, H.C., Buchner, P., Lahner, B., Danku, J., Zhao, K., Lee, J., Hawkesford, M.J., Guerinot, M.L., and Salt, D.E. (2008). Variation in molybdenum content across broadly distributed populations of Arabidopsis thaliana is controlled by a mitochondrial molybdenum transporter (MOT1;1). *PLoS Genet.* 4, e1000004.

Pubmed: [Author and Title](#)

CrossRef: [Author and Title](#)

Google Scholar: [Author Only](#) [Title Only](#) [Author and Title](#)

Baxter, I., Brazelton, J.N., Yu, D., Huang, Y.S., Lahner, B., Yakubova, E., Li, Y., Bergelson, J., Borevitz, J.O., Nordborg, M., Vitek, O., and Salt, D.E. (2010). A coastal cline in sodium accumulation in Arabidopsis thaliana is driven by natural variation of the sodium transporter AtHKT1;1. *PLoS Genet.* 6, e1001193.

Pubmed: [Author and Title](#)

CrossRef: [Author and Title](#)

Google Scholar: [Author Only](#) [Title Only](#) [Author and Title](#)

Bradbury, P.J., Zhang, Z., Kroon, D.E., Casstevens, T.M., Ramdoss, Y., and Buckler, E.S. (2007). TASSEL: software for association mapping of complex traits in diverse samples. *Bioinformatics* 23, 2633-2635.

Pubmed: [Author and Title](#)

CrossRef: [Author and Title](#)

Google Scholar: [Author Only](#) [Title Only](#) [Author and Title](#)

Chao, D.Y., Silva, A., Baxter, I., Huang, Y.S., Nordborg, M., Danku, J., Lahner, B., Yakubova, E., and Salt, D.E. (2012). Genome-Wide Association Studies Identify Heavy Metal ATPase3 as the Primary Determinant of Natural Variation in Leaf Cadmium in Arabidopsis thaliana. *PLoS Genet.* 8.

Pubmed: [Author and Title](#)

CrossRef: [Author and Title](#)

Google Scholar: [Author Only](#) [Title Only](#) [Author and Title](#)

Chao, D.Y., Chen, Y., Chen, J., Shi, S., Chen, Z., Wang, C., Danku, J.M., Zhao, F.J., and Salt, D.E. (2014). Genome-wide association mapping identifies a new arsenate reductase enzyme critical for limiting arsenic accumulation in plants. *PLoS Biol.* 12, e1002009.

Pubmed: [Author and Title](#)

CrossRef: [Author and Title](#)

Google Scholar: [Author Only](#) [Title Only](#) [Author and Title](#)

Chen, H., Tang, Z., Wang, P., and Zhao, F.J. (2018). Geographical variations of cadmium and arsenic concentrations and arsenic speciation in Chinese rice. *Environ. Pollut.* 238, 482-490.

Pubmed: [Author and Title](#)

CrossRef: [Author and Title](#)

Google Scholar: [Author Only](#) [Title Only](#) [Author and Title](#)

- Chen, W., et al. (2014). Genome-wide association analyses provide genetic and biochemical insights into natural variation in rice metabolism. *Nat. Genet.* 46, 714-721.**
Pubmed: [Author and Title](#)
CrossRef: [Author and Title](#)
Google Scholar: [Author Only Title Only Author and Title](#)
- Chen, W., Wang, W., Peng, M., Gong, L., Gao, Y., Wan, J., Wang, S., Shi, L., Zhou, B., Li, Z., Peng, X., Yang, C., Qu, L., Liu, X., and Luo, J. (2016). Comparative and parallel genome-wide association studies for metabolic and agronomic traits in cereals. *Nat Commun* 7, 12767.**
Pubmed: [Author and Title](#)
CrossRef: [Author and Title](#)
Google Scholar: [Author Only Title Only Author and Title](#)
- Clemens, S., and Ma, J.F. (2016). Toxic Heavy Metal and Metalloid Accumulation in Crop Plants and Foods. *Annu. Rev. Plant Biol.* 67, 489-512.**
Pubmed: [Author and Title](#)
CrossRef: [Author and Title](#)
Google Scholar: [Author Only Title Only Author and Title](#)
- Clemens, S., Palmgren, M.G., and Kramer, U. (2002). A long way ahead: understanding and engineering plant metal accumulation. *Trends Plant Sci.* 7, 309-315.**
Pubmed: [Author and Title](#)
CrossRef: [Author and Title](#)
Google Scholar: [Author Only Title Only Author and Title](#)
- Cotsaftis, O., Plett, D., Shirley, N., Tester, M., and Hrmova, M. (2012). A two-staged model of Na⁺ exclusion in rice explained by 3D modeling of HKT transporters and alternative splicing. *PLoS One* 7, e39865.**
Pubmed: [Author and Title](#)
CrossRef: [Author and Title](#)
Google Scholar: [Author Only Title Only Author and Title](#)
- Du, J., Zeng, D., Wang, B., Qian, Q., Zheng, S., and Ling, H.Q. (2013). Environmental effects on mineral accumulation in rice grains and identification of ecological specific QTLs. *Environ. Geochem. Health* 35, 161-170.**
Pubmed: [Author and Title](#)
CrossRef: [Author and Title](#)
Google Scholar: [Author Only Title Only Author and Title](#)
- Duan, G.L., Shao, G.S., Tang, Z., Chen, H.P., Wang, B.X., Tang, Z., Yang, Y.P., Liu, Y.C., and Zhao, F.J. (2017). Genotypic and Environmental Variations in Grain Cadmium and Arsenic Concentrations Among a Panel of High Yielding Rice Cultivars. *Rice* 10.**
Pubmed: [Author and Title](#)
CrossRef: [Author and Title](#)
Google Scholar: [Author Only Title Only Author and Title](#)
- Famoso, A.N., Zhao, K., Clark, R.T., Tung, C.W., Wright, M.H., Bustamante, C., Kochian, L.V., and McCouch, S.R. (2011). Genetic Architecture of Aluminum Tolerance in Rice (*Oryza sativa*) Determined through Genome-Wide Association Analysis and QTL Mapping. *PLoS Genet.* 7.**
Pubmed: [Author and Title](#)
CrossRef: [Author and Title](#)
Google Scholar: [Author Only Title Only Author and Title](#)
- Forsberg, S.K., Andreatta, M.E., Huang, X.Y., Danku, J., Salt, D.E., and Carlborg, O. (2015). The Multi-allelic Genetic Architecture of a Variance-Heterogeneity Locus for Molybdenum Concentration in Leaves Acts as a Source of Unexplained Additive Genetic Variance. *PLoS Genet.* 11, e1005648.**
Pubmed: [Author and Title](#)
CrossRef: [Author and Title](#)
Google Scholar: [Author Only Title Only Author and Title](#)
- Garcia-Oliveira, A.L., Tan, L., Fu, Y., and Sun, C. (2009). Genetic identification of quantitative trait loci for contents of mineral nutrients in rice grain. *J. Integr. Plant Biol.* 51, 84-92.**
Pubmed: [Author and Title](#)
CrossRef: [Author and Title](#)
Google Scholar: [Author Only Title Only Author and Title](#)
- Hermans, C., Hammond, J.P., White, P.J., and Verbruggen, N. (2006). How do plants respond to nutrient shortage by biomass allocation? *Trends Plant Sci.* 11, 610-617.**
Pubmed: [Author and Title](#)
CrossRef: [Author and Title](#)
Google Scholar: [Author Only Title Only Author and Title](#)
- Hirel, B., Le Gouis, J., Ney, B., and Gallais, A. (2007). The challenge of improving nitrogen use efficiency in crop plants: towards a more central role for genetic variability and quantitative genetics within integrated approaches. *J. Exp. Bot.* 58, 2369-2387.**
Pubmed: [Author and Title](#)
CrossRef: [Author and Title](#)
Google Scholar: [Author Only Title Only Author and Title](#)
- Horie, T., Hauser, F., and Schroeder, J.I. (2009). HKT transporter-mediated salinity resistance mechanisms in *Arabidopsis* and monocot**

crop plants. Trends Plant Sci. 14, 660-668.

Pubmed: [Author and Title](#)

CrossRef: [Author and Title](#)

Google Scholar: [Author Only Title Only Author and Title](#)

Hu, B., et al. (2015). Variation in NRT1.1B contributes to nitrate-use divergence between rice subspecies. Nat. Genet.

Pubmed: [Author and Title](#)

CrossRef: [Author and Title](#)

Google Scholar: [Author Only Title Only Author and Title](#)

Huang, X., et al. (2012a). Genome-wide association study of flowering time and grain yield traits in a worldwide collection of rice germplasm. Nat. Genet. 44, 32-39.

Pubmed: [Author and Title](#)

CrossRef: [Author and Title](#)

Google Scholar: [Author Only Title Only Author and Title](#)

Huang, X., et al. (2012b). A map of rice genome variation reveals the origin of cultivated rice. Nature 490, 497-501.

Pubmed: [Author and Title](#)

CrossRef: [Author and Title](#)

Google Scholar: [Author Only Title Only Author and Title](#)

Huang, X.H., and Han, B. (2014). Natural Variations and Genome-Wide Association Studies in Crop Plants. Annu. Rev. Plant Biol. 65, 531-551.

Pubmed: [Author and Title](#)

CrossRef: [Author and Title](#)

Google Scholar: [Author Only Title Only Author and Title](#)

Huang, X.H., et al. (2010). Genome-wide association studies of 14 agronomic traits in rice landraces. Nat. Genet. 42, 961-U976.

Pubmed: [Author and Title](#)

CrossRef: [Author and Title](#)

Google Scholar: [Author Only Title Only Author and Title](#)

Huang, X.Y., and Salt, D.E. (2016). Plant Ionomics: From Elemental Profiling to Environmental Adaptation. Mol Plant 9, 787-797.

Pubmed: [Author and Title](#)

CrossRef: [Author and Title](#)

Google Scholar: [Author Only Title Only Author and Title](#)

Huang, X.Y., Deng, F., Yamaji, N., Pinson, S.R., Fujii-Kashino, M., Danku, J., Douglas, A., Guerinot, M.L., Salt, D.E., and Ma, J.F. (2016). A heavy metal P-type ATPase OshMA4 prevents copper accumulation in rice grain. Nat Commun 7, 12138.

Pubmed: [Author and Title](#)

CrossRef: [Author and Title](#)

Google Scholar: [Author Only Title Only Author and Title](#)

Jiao, Y., Wang, Y., Xue, D., Wang, J., Yan, M., Liu, G., Dong, G., Zeng, D., Lu, Z., Zhu, X., Qian, Q., and Li, J. (2010). Regulation of OsSPL14 by OsmiR156 defines ideal plant architecture in rice. Nat. Genet. 42, 541-544.

Pubmed: [Author and Title](#)

CrossRef: [Author and Title](#)

Google Scholar: [Author Only Title Only Author and Title](#)

Jung, C., and Muller, A.E. (2009). Flowering time control and applications in plant breeding. Trends Plant Sci. 14, 563-573.

Pubmed: [Author and Title](#)

CrossRef: [Author and Title](#)

Google Scholar: [Author Only Title Only Author and Title](#)

Lahner, B., Gong, J.M., Mahmoudian, M., Smith, E.L., Abid, K.B., Rogers, E.E., Guerinot, M.L., Harper, J.F., Ward, J.M., McIntyre, L., Schroeder, J.I., and Salt, D.E. (2003). Genomic scale profiling of nutrient and trace elements in Arabidopsis thaliana. Nat. Biotechnol. 21, 1215-1221.

Pubmed: [Author and Title](#)

CrossRef: [Author and Title](#)

Google Scholar: [Author Only Title Only Author and Title](#)

Li, M.X., Yeung, J.M., Cherny, S.S., and Sham, P.C. (2012). Evaluating the effective numbers of independent tests and significant p-value thresholds in commercial genotyping arrays and public imputation reference datasets. Hum. Genet. 131, 747-756.

Pubmed: [Author and Title](#)

CrossRef: [Author and Title](#)

Google Scholar: [Author Only Title Only Author and Title](#)

Liu, C., Chen, G., Li, Y., Peng, Y., Zhang, A., Hong, K., Jiang, H., Ruan, B., Zhang, B., Yang, S., Gao, Z., and Qian, Q. (2017). Characterization of a major QTL for manganese accumulation in rice grain. Sci. Rep. 7, 17704.

Pubmed: [Author and Title](#)

CrossRef: [Author and Title](#)

Google Scholar: [Author Only Title Only Author and Title](#)

Livak, K.J., and Schmittgen, T.D. (2001). Analysis of relative gene expression data using real-time quantitative PCR and the 2(-Delta Delta C(T)) Method. Methods 25, 402-408.

Pubmed: [Author and Title](#)

- CrossRef: [Author and Title](#)
Google Scholar: [Author Only Title Only Author and Title](#)
- Lu, K.Y., Li, L.Z., Zheng, X.F., Zhang, Z.H., Mou, T.M., and Hu, Z.L. (2008).** Quantitative trait loci controlling Cu, Ca, Zn, Mn and Fe content in rice grains. *J Genet* 87, 305-310.
Pubmed: [Author and Title](#)
CrossRef: [Author and Title](#)
Google Scholar: [Author Only Title Only Author and Title](#)
- Lu, L., Yan, W., Xue, W., Shao, D., and Xing, Y. (2012).** Evolution and association analysis of Ghd7 in rice. *PLoS One* 7, e34021.
Pubmed: [Author and Title](#)
CrossRef: [Author and Title](#)
Google Scholar: [Author Only Title Only Author and Title](#)
- Mahender, A., Anandan, A., Pradhan, S.K., and Pandit, E. (2016).** Rice grain nutritional traits and their enhancement using relevant genes and QTLs through advanced approaches. Springerplus 5.
Pubmed: [Author and Title](#)
CrossRef: [Author and Title](#)
Google Scholar: [Author Only Title Only Author and Title](#)
- Marschner, H., and Marschner, P. (2012).** Marschner's mineral nutrition of higher plants. (London ; Waltham, MA: Elsevier/Academic Press).
Pubmed: [Author and Title](#)
CrossRef: [Author and Title](#)
Google Scholar: [Author Only Title Only Author and Title](#)
- Matsuda, F., Nakabayashi, R., Yang, Z., Okazaki, Y., Yonemaru, J., Ebana, K., Yano, M., and Saito, K. (2015).** Metabolome-genome-wide association study dissects genetic architecture for generating natural variation in rice secondary metabolism. *Plant J.* 81, 13-23.
Pubmed: [Author and Title](#)
CrossRef: [Author and Title](#)
Google Scholar: [Author Only Title Only Author and Title](#)
- Matsumoto, T., et al. (2005).** The map-based sequence of the rice genome. *Nature* 436, 793-800.
Pubmed: [Author and Title](#)
CrossRef: [Author and Title](#)
Google Scholar: [Author Only Title Only Author and Title](#)
- McNally, K.L., et al. (2009).** Genomewide SNP variation reveals relationships among landraces and modern varieties of rice. *Proc. Natl. Acad. Sci. U. S. A.* 106, 12273-12278.
Pubmed: [Author and Title](#)
CrossRef: [Author and Title](#)
Google Scholar: [Author Only Title Only Author and Title](#)
- Ming, R., Del Monte, T.A., Hernandez, E., Moore, P.H., Irvine, J.E., and Paterson, A.H. (2002).** Comparative analysis of QTLs affecting plant height and flowering among closely-related diploid and polyploid genomes. *Genome* 45, 794-803.
Pubmed: [Author and Title](#)
CrossRef: [Author and Title](#)
Google Scholar: [Author Only Title Only Author and Title](#)
- Miyadate, H., Adachi, S., Hiraizumi, A., Tezuka, K., Nakazawa, N., Kawamoto, T., Katou, K., Kodama, I., Sakurai, K., Takahashi, H., Satoh-Nagasawa, N., Watanabe, A., Fujimura, T., and Akagi, H. (2011).** OsHMA3, a P-1B-type of ATPase affects root-to-shoot cadmium translocation in rice by mediating efflux into vacuoles. *New Phytol.* 189, 190-199.
Pubmed: [Author and Title](#)
CrossRef: [Author and Title](#)
Google Scholar: [Author Only Title Only Author and Title](#)
- Morrissey, J., Baxter, I.R., Lee, J., Li, L.T., Lahner, B., Grotz, N., Kaplan, J., Salt, D.E., and Guerinot, M.L. (2009).** The Ferroportin Metal Efflux Proteins Function in Iron and Cobalt Homeostasis in Arabidopsis. *Plant Cell* 21, 3326-3338.
Pubmed: [Author and Title](#)
CrossRef: [Author and Title](#)
Google Scholar: [Author Only Title Only Author and Title](#)
- Munns, R., James, R.A., Xu, B., Athman, A., Conn, S.J., Jordans, C., Byrt, C.S., Hare, R.A., Tyerman, S.D., Tester, M., Plett, D., and Gilliam, M. (2012).** Wheat grain yield on saline soils is improved by an ancestral Na⁺ transporter gene. *Nat. Biotechnol.* 30, 360-U173.
Pubmed: [Author and Title](#)
CrossRef: [Author and Title](#)
Google Scholar: [Author Only Title Only Author and Title](#)
- Nawaz, Z., Kakar, K.U., Li, X.B., Li, S., Zhang, B., Shou, H.X., and Shu, Q.Y. (2015).** Genome-wide Association Mapping of Quantitative Trait Loci (QTLs) for Contents of Eight Elements in Brown Rice (*Oryza sativa* L.). *J. Agric. Food Chem.* 63, 8008-8016.
Pubmed: [Author and Title](#)
CrossRef: [Author and Title](#)
Google Scholar: [Author Only Title Only Author and Title](#)
- Negrao, S., Almadanim, M.C., Pires, I.S., Abreu, I.A., Maroco, J., Courtois, B., Gregorio, G.B., McNally, K.L., and Oliveira, M.M. (2013).** New allelic variants found in key rice salt-tolerance genes: an association study. *Plant Biotechnol. J.* 11, 87-100.

Pubmed: [Author and Title](#)
CrossRef: [Author and Title](#)
Google Scholar: [Author Only Title Only Author and Title](#)

Norton, G.J., Deacon, C.M., Xiong, L.Z., Huang, S.Y., Meharg, A.A., and Price, A.H. (2010). Genetic mapping of the rice ionome in leaves and grain: identification of QTLs for 17 elements including arsenic, cadmium, iron and selenium. Plant Soil 329, 139-153.

Pubmed: [Author and Title](#)
CrossRef: [Author and Title](#)
Google Scholar: [Author Only Title Only Author and Title](#)

Norton, G.J., Duan, G.L., Lei, M., Zhu, Y.G., Meharg, A.A., and Price, A.H. (2012a). Identification of quantitative trait loci for rice grain element composition on an arsenic impacted soil: Influence of flowering time on genetic loci. Ann. Appl. Biol. 161, 46-56.

Pubmed: [Author and Title](#)
CrossRef: [Author and Title](#)
Google Scholar: [Author Only Title Only Author and Title](#)

Norton, G.J., et al. (2012b). Variation in grain arsenic assessed in a diverse panel of rice (*Oryza sativa*) grown in multiple sites. New Phytol. 193, 650-664.

Pubmed: [Author and Title](#)
CrossRef: [Author and Title](#)
Google Scholar: [Author Only Title Only Author and Title](#)

Norton, G.J., et al. (2014). Genome Wide Association Mapping of Grain Arsenic, Copper, Molybdenum and Zinc in Rice (*Oryza sativa* L.) Grown at Four International Field Sites. PLoS One 9, e89685.

Pubmed: [Author and Title](#)
CrossRef: [Author and Title](#)
Google Scholar: [Author Only Title Only Author and Title](#)

Ohmori, Y., Sotta, N., and Fujiwara, T. (2016). Identification of introgression lines of *Oryza glaberrima* Steud. with high mineral content in grains. Soil Sci. Plant Nutr. 62, 456-464.

Pubmed: [Author and Title](#)
CrossRef: [Author and Title](#)
Google Scholar: [Author Only Title Only Author and Title](#)

Palmgren, M.G. (2001). PLANT PLASMA MEMBRANE H⁺-ATPases: Powerhouses for Nutrient Uptake. Annu. Rev. Plant Physiol. Plant Mol. Biol. 52, 817-845.

Pubmed: [Author and Title](#)
CrossRef: [Author and Title](#)
Google Scholar: [Author Only Title Only Author and Title](#)

Paterson, A.H., Lin, Y.R., Li, Z., Schertz, K.F., Doebley, J.F., Pinson, S.R., Liu, S.C., Stansel, J.W., and Irvine, J.E. (1995). Convergent domestication of cereal crops by independent mutations at corresponding genetic Loci. Science 269, 1714-1718.

Pubmed: [Author and Title](#)
CrossRef: [Author and Title](#)
Google Scholar: [Author Only Title Only Author and Title](#)

Platten, J.D., Egdane, J.A., and Ismail, A.M. (2013). Salinity tolerance, Na⁺ exclusion and allele mining of HKT1;5 in *Oryza sativa* and *O. glaberrima*: many sources, many genes, one mechanism? BMC Plant Biol. 13, 32.

Pubmed: [Author and Title](#)
CrossRef: [Author and Title](#)
Google Scholar: [Author Only Title Only Author and Title](#)

Pinson, S.R.M., Tarpley, L., Yan, W.G., Yeater, K., Lahner, B., Yakubova, E., Huang, X.Y., Zhang, M., Guerinot, M.L., and Salt, D.E. (2015). Worldwide Genetic Diversity for Mineral Element Concentrations in Rice Grain. Crop Sci. 55, 294-311.

Pubmed: [Author and Title](#)
CrossRef: [Author and Title](#)
Google Scholar: [Author Only Title Only Author and Title](#)

Ren, Z.H., Gao, J.P., Li, L.G., Cai, X.L., Huang, W., Chao, D.Y., Zhu, M.Z., Wang, Z.Y., Luan, S., and Lin, H.X. (2005). A rice quantitative trait locus for salt tolerance encodes a sodium transporter. Nat. Genet. 37, 1141-1146.

Pubmed: [Author and Title](#)
CrossRef: [Author and Title](#)
Google Scholar: [Author Only Title Only Author and Title](#)

Salt, D.E., Baxter, I., and Lahner, B. (2008). Ionomics and the study of the plant ionome. Annual Review of Plant Biology, Vol 63 59, 709-733.

Pubmed: [Author and Title](#)
CrossRef: [Author and Title](#)
Google Scholar: [Author Only Title Only Author and Title](#)

Sasaki, A., Yamaji, N., Yokosho, K., and Ma, J.F. (2012). Nramp5 is a major transporter responsible for manganese and cadmium uptake in rice. Plant Cell 24, 2155-2167.

Pubmed: [Author and Title](#)
CrossRef: [Author and Title](#)
Google Scholar: [Author Only Title Only Author and Title](#)

Segura, V., Vilhjalmsón, B.J., Platt, A., Korte, A., Seren, U., Long, Q., and Nordborg, M. (2012). An efficient multi-locus mixed-model approach for genome-wide association studies in structured populations. *Nat. Genet.* 44, 825-830.

Pubmed: [Author and Title](#)

CrossRef: [Author and Title](#)

Google Scholar: [Author Only Title Only Author and Title](#)

Seren, U., Vilhjalmsón, B.J., Horton, M.W., Meng, D., Forai, P., Huang, Y.S., Long, Q., Segura, V., and Nordborg, M. (2012). GWAPP: a web application for genome-wide association mapping in Arabidopsis. *Plant Cell* 24, 4793-4805.

Pubmed: [Author and Title](#)

CrossRef: [Author and Title](#)

Google Scholar: [Author Only Title Only Author and Title](#)

Shen, X., Pettersson, M., Ronnegard, L., and Carlborg, O. (2012). Inheritance beyond plain heritability: variance-controlling genes in *Arabidopsis thaliana*. *PLoS Genet.* 8, e1002839.

Pubmed: [Author and Title](#)

CrossRef: [Author and Title](#)

Google Scholar: [Author Only Title Only Author and Title](#)

Si, L., et al. (2016). OsSPL13 controls grain size in cultivated rice. *Nat. Genet.* 48, 447-456.

Pubmed: [Author and Title](#)

CrossRef: [Author and Title](#)

Google Scholar: [Author Only Title Only Author and Title](#)

Sun, H., et al. (2014). Heterotrimeric G proteins regulate nitrogen-use efficiency in rice. *Nat. Genet.*

Pubmed: [Author and Title](#)

CrossRef: [Author and Title](#)

Google Scholar: [Author Only Title Only Author and Title](#)

Swamy, B.P.M., Rahman, M.A., Inabangan-Asilo, M.A., Amparado, A., Manito, C., Chadha-Mohanty, P., Reinke, R., and Slamet-Loedin, I.H. (2016). Advances in breeding for high grain Zinc in Rice. *Rice (N Y)* 9, 49.

Pubmed: [Author and Title](#)

CrossRef: [Author and Title](#)

Google Scholar: [Author Only Title Only Author and Title](#)

Tomatsu, H., Takano, J., Takahashi, H., Watanabe-Takahashi, A., Shibagaki, N., and Fujiwara, T. (2007). An *Arabidopsis thaliana* high-affinity molybdate transporter required for efficient uptake of molybdate from soil. *Proc. Natl. Acad. Sci. U. S. A.* 104, 18807-18812.

Pubmed: [Author and Title](#)

CrossRef: [Author and Title](#)

Google Scholar: [Author Only Title Only Author and Title](#)

Tomcal, M., Stiffler, N., and Barkan, A. (2013). POGs2: a web portal to facilitate cross-species inferences about protein architecture and function in plants. *PLoS One* 8, e82569.

Pubmed: [Author and Title](#)

CrossRef: [Author and Title](#)

Google Scholar: [Author Only Title Only Author and Title](#)

Trijatmiko, K.R., et al. (2016). Biofortified indica rice attains iron and zinc nutrition dietary targets in the field. *Sci. Rep.* 6, 19792.

Pubmed: [Author and Title](#)

CrossRef: [Author and Title](#)

Google Scholar: [Author Only Title Only Author and Title](#)

Ueno, D., Yamaji, N., Kono, I., Huang, C.F., Ando, T., Yano, M., and Ma, J.F. (2010). Gene limiting cadmium accumulation in rice. *Proc. Natl. Acad. Sci. U. S. A.* 107, 16500-16505.

Pubmed: [Author and Title](#)

CrossRef: [Author and Title](#)

Google Scholar: [Author Only Title Only Author and Title](#)

Ueno, D., Milner, M.J., Yamaji, N., Yokosho, K., Koyama, E., Clemencia Zambrano, M., Kaskie, M., Ebbs, S., Kochian, L.V., and Ma, J.F. (2011). Elevated expression of TcHMA3 plays a key role in the extreme Cd tolerance in a Cd-hyperaccumulating ecotype of *Thlaspi caerulescens*. *Plant J.* 66, 852-862.

Pubmed: [Author and Title](#)

CrossRef: [Author and Title](#)

Google Scholar: [Author Only Title Only Author and Title](#)

Uraguchi, S., and Fujiwara, T. (2013). Rice breaks ground for cadmium-free cereals. *Curr. Opin. Plant Biol.* 16, 328-334.

Pubmed: [Author and Title](#)

CrossRef: [Author and Title](#)

Google Scholar: [Author Only Title Only Author and Title](#)

Van Bel, M., Proost, S., Wischnitzki, E., Movahedi, S., Scheerlinck, C., Van de Peer, Y., and Vandepoele, K. (2012). Dissecting plant genomes with the PLAZA comparative genomics platform. *Plant Physiol.* 158, 590-600.

Pubmed: [Author and Title](#)

CrossRef: [Author and Title](#)

Google Scholar: [Author Only Title Only Author and Title](#)

Wang, Q., Xie, W., Xing, H., Yan, J., Meng, X., Li, X., Fu, X., Xu, J., Lian, X., Yu, S., Xing, Y., and Wang, G. (2015). Genetic architecture of natural variation in rice chlorophyll content revealed by genome wide association study. *Mol Plant*.

Pubmed: [Author and Title](#)

CrossRef: [Author and Title](#)

Google Scholar: [Author Only Title Only Author and Title](#)

Wei, D., Cui, K.H., Ye, G.Y., Pan, J.F., Xiang, J., Huang, J.L., and Nie, L.X. (2012). QTL mapping for nitrogen-use efficiency and nitrogen-deficiency tolerance traits in rice. *Plant Soil* 359, 281-295.

Pubmed: [Author and Title](#)

CrossRef: [Author and Title](#)

Google Scholar: [Author Only Title Only Author and Title](#)

Wei, X.J., Xu, J.F., Guo, H.N., Jiang, L., Chen, S.H., Yu, C.Y., Zhou, Z.L., Hu, P.S., Zhai, H.Q., and Wan, J.M. (2010). DTH8 Suppresses Flowering in Rice, Influencing Plant Height and Yield Potential Simultaneously. *Plant Physiol.* 153, 1747-1758.

Pubmed: [Author and Title](#)

CrossRef: [Author and Title](#)

Google Scholar: [Author Only Title Only Author and Title](#)

Weng, X.Y., Wang, L., Wang, J., Hu, Y., Du, H., Xu, C.G., Xing, Y.Z., Li, X.H., Xiao, J.H., and Zhang, Q.F. (2014). Grain Number, Plant Height, and Heading Date7 Is a Central Regulator of Growth, Development, and Stress Response. *Plant Physiol.* 164, 735-747.

Pubmed: [Author and Title](#)

CrossRef: [Author and Title](#)

Google Scholar: [Author Only Title Only Author and Title](#)

White, P.J., and Broadley, M.R. (2009). Biofortification of crops with seven mineral elements often lacking in human diets - iron, zinc, copper, calcium, magnesium, selenium and iodine. *New Phytol.* 182, 49-84.

Pubmed: [Author and Title](#)

CrossRef: [Author and Title](#)

Google Scholar: [Author Only Title Only Author and Title](#)

Williams, L., and Salt, D.E. (2009). The plant ionome coming into focus. *Curr. Opin. Plant Biol.* 12, 247-249.

Pubmed: [Author and Title](#)

CrossRef: [Author and Title](#)

Google Scholar: [Author Only Title Only Author and Title](#)

Withers, P.J.A., and Lord, E.I. (2002). Agricultural nutrient inputs to rivers and groundwaters in the UK: policy, environmental management and research needs. *Sci. Total Environ.* 282, 9-24.

Pubmed: [Author and Title](#)

CrossRef: [Author and Title](#)

Google Scholar: [Author Only Title Only Author and Title](#)

Xie, W., et al. (2015). Breeding signatures of rice improvement revealed by a genomic variation map from a large germplasm collection. *Proc. Natl. Acad. Sci. U. S. A* 112, E5411-5419.

Pubmed: [Author and Title](#)

CrossRef: [Author and Title](#)

Google Scholar: [Author Only Title Only Author and Title](#)

Xue, W.Y., Xing, Y.Z., Weng, X.Y., Zhao, Y., Tang, W.J., Wang, L., Zhou, H.J., Yu, S.B., Xu, C.G., Li, X.H., and Zhang, Q.F. (2008). Natural variation in Ghd7 is an important regulator of heading date and yield potential in rice. *Nat. Genet.* 40, 761-767.

Pubmed: [Author and Title](#)

CrossRef: [Author and Title](#)

Google Scholar: [Author Only Title Only Author and Title](#)

Yan, W.H., Wang, P., Chen, H.X., Zhou, H.J., Li, Q.P., Wang, C.R., Ding, Z.H., Zhang, Y.S., Yu, S.B., Xing, Y.Z., and Zhang, Q.F. (2011). A major QTL, Ghd8, plays pleiotropic roles in regulating grain productivity, plant height, and heading date in rice. *Molecular plant* 4, 319-330.

Pubmed: [Author and Title](#)

CrossRef: [Author and Title](#)

Google Scholar: [Author Only Title Only Author and Title](#)

Yang, M., Zhang, Y., Zhang, L., Hu, J., Zhang, X., Lu, K., Dong, H., Wang, D., Zhao, F.J., Huang, C.F., and Lian, X. (2014). OsNRAMP5 contributes to manganese translocation and distribution in rice shoots. *J. Exp. Bot.* 65, 4849-4861.

Pubmed: [Author and Title](#)

CrossRef: [Author and Title](#)

Google Scholar: [Author Only Title Only Author and Title](#)

Yano, K., Yamamoto, E., Aya, K., Takeuchi, H., Lo, P.C., Hu, L., Yamasaki, M., Yoshida, S., Kitano, H., Hirano, K., and Matsuoka, M. (2016). Genome-wide association study using whole-genome sequencing rapidly identifies new genes influencing agronomic traits in rice. *Nat. Genet.* 48, 927-934.

Pubmed: [Author and Title](#)

CrossRef: [Author and Title](#)

Google Scholar: [Author Only Title Only Author and Title](#)

Yoshida, S., Forno, D.A., Cock, J.H., and Gomez, K.A. (1976). Laboratory Manual for Physiological Studies of Rice, 3rd ed. International Rice Research Institute, Manila.

Pubmed: [Author and Title](#)
CrossRef: [Author and Title](#)
Google Scholar: [Author Only](#) [Title Only](#) [Author and Title](#)

Yu, S.B., Xu, W.J., Vijayakumar, C.H., Ali, J., Fu, B.Y., Xu, J.L., Jiang, Y.Z., Marghirang, R., Domingo, J., Aquino, C., Virmani, S.S., and Li, Z.K. (2003). Molecular diversity and multilocus organization of the parental lines used in the International Rice Molecular Breeding Program. *Theor. Appl. Genet.* 108, 131-140.

Pubmed: [Author and Title](#)
CrossRef: [Author and Title](#)
Google Scholar: [Author Only](#) [Title Only](#) [Author and Title](#)

Zhang, H., Zhang, D., Wang, M., Sun, J., Qi, Y., Li, J., Wei, X., Han, L., Qiu, Z., Tang, S., and Li, Z (2011). A core collection and mini core collection of *Oryza sativa* L. in China. *Theor. Appl. Genet.* 122, 49-61.

Pubmed: [Author and Title](#)
CrossRef: [Author and Title](#)
Google Scholar: [Author Only](#) [Title Only](#) [Author and Title](#)

Zhang, M., Pinson, S.R., Tarpley, L., Huang, X.Y., Lahner, B., Yakubova, E., Baxter, I., Guerinot, M.L., and Salt, D.E. (2014). Mapping and validation of quantitative trait loci associated with concentrations of 16 elements in unmilled rice grain. *Theor. Appl. Genet.* 127, 137-165.

Pubmed: [Author and Title](#)
CrossRef: [Author and Title](#)
Google Scholar: [Author Only](#) [Title Only](#) [Author and Title](#)

Zhang, J., et al. (2015). Combinations of the Ghd7, Ghd8 and Hd1 genes largely define the ecogeographical adaptation and yield potential of cultivated rice. *New Phytol.* 208, 1056-1066.

Pubmed: [Author and Title](#)
CrossRef: [Author and Title](#)
Google Scholar: [Author Only](#) [Title Only](#) [Author and Title](#)

Zhao, F.J., McGrath, S.P., and Meharg, A.A. (2010). Arsenic as a Food Chain Contaminant: Mechanisms of Plant Uptake and Metabolism and Mitigation Strategies. *Annu. Rev. Plant Biol.* 61, 535-559.

Pubmed: [Author and Title](#)
CrossRef: [Author and Title](#)
Google Scholar: [Author Only](#) [Title Only](#) [Author and Title](#)

Zhao, H., Yao, W., Ouyang, Y., Yang, W., Wang, G., Lian, X., Xing, Y., Chen, L., and Xie, W. (2014). RiceVarMap: a comprehensive database of rice genomic variations. *Nucleic Acids Res.*

Pubmed: [Author and Title](#)
CrossRef: [Author and Title](#)
Google Scholar: [Author Only](#) [Title Only](#) [Author and Title](#)